restriction HLA allotypes target distinct intervals of HIV-1 pathogenesis. Nat. Med. 11:1290–1292. http://dx.doi.org/10.1038/nm1333.
39. Kelleher AD, Long C, Holmes EC, Allen RL, Wilson J, Conlon C, Workman C, Shaunak S, Olson K, Goulder P, Brander C, Ogg G, Sullivan JS, Dyer W, Jones I, McMichael AJ, Rowland-Jones S, Phillips RE. 2001. Clustered mutations in HIV-1 gag are consistently required for escape from HLA-B27-restricted cytotoxic T lymphocyte responses. J. Exp. Med. 193:375–386. http://dx.doi.org/10.1084/jem.193.3.375.
40. Leslie AJ, Pfafferott KJ, Chetty P, Draenert R, Addo MM, Feeney M, Tang Y, Holmes EC, Allen T, Prado JG, Altfeld M, Brander C, Dixon C, Ramduth D, Jeena P, Thomas SA, St John A, Roach TA, Kupfer B, Luzzi G, Edwards A, Taylor G, Lyall H, Tudor-Williams G, Novelli V, Martinez-Picado J, Kiepiela P, Walker BD, Goulder PJ. 2004. HIV evolution: CTL escape mutation and reversion after transmission. Nat. Med. 10:282–289. http://dx.doi.org/10.1038/nm992.
41. Schneidewind A, Brockman MA, Yang R, Adam RI, Li B, Le Gall S, Rinaldo CR, Craggs SL, Allgaier RL, Power KA, Kuntzen T, Tung CS, LaBute MX, Mueller SM, Harrer T, McMichael AJ, Goulder PJ, Aiken C, Brander C, Kelleher AD, Allen TM. 2007. Escape from the dominant HLA-B27-restricted cytotoxic T-lymphocyte response in Gag is associated with a dramatic reduction in human immunodeficiency virus type 1 replication. J. Virol. 81:12382–12393. http://dx.doi.org/10.1128/JVI.01543-07.
42. Chopera DR, Woodman Z, Mlisana K, Mlotshwa M, Martin DP, Seoighe C, Treurnicht F, de Rosa DA, Hide W, Karim SA, Gray CM, Williamson C, CAPRISA 002 Study Team, . 2008. Transmission of HIV-1 CTL escape variants provides HLA-mismatched recipients with a survival advantage. PLoS Pathog. 4:e1000033. http://dx.doi.org/10.1371/journal.ppat.1000033.
43. Goepfert PA, Lumm W, Farmer P, Matthews P, Prendergast A, Carlson JM, Derdeyn CA, Tang J, Kaslow RA, Bansal A, Yusim K, Heckerman D, Mulenga J, Allen S, Goulder PJ, Hunter E. 2008. Transmission of HIV-1 Gag immune escape mutations is associated with reduced viral load in linked recipients. J. Exp. Med. 205:1009–1017. http://dx.doi.org/10.1084/jem.20072457.
44. Vivian JP, Duncan RC, Berry R, O'Connor GM, Reid HH, Beddoe T, Gras S, Saunders PM, Olshina MA, Widjaja JM, Harpur CM, Lin J, Maloveste SM, Price DA, Lafont BA, McVicar DW, Clements CS, Brooks AG, Rossjohn J. 2011. Killer cell immunoglobulin-like receptor 3DL1-mediated recognition of human leukocyte antigen B. Nature 479:401–405. http://dx.doi.org/10.1038/nature10517.
45. Apps R, Qi Y, Carlson JM, Chen H, Gao X, Thomas R, Yuki Y, Del Prete GQ, Goulder P, Brumme ZL, Brumme CJ, John M, Mallal S, Nelson G, Bosch R, Heckerman D, Stein JL, Soderberg KA, Moody MA, Denny TN, Zeng X, Fang J, Moffett A, Lifson JD, Goedert JJ, Buchbinder S, Kirk GD, Fellay J, McLaren P, Deeks SG, Pereyra F, Walker B, Michael NL, Weintrob A, Wolinsky S, Liao W, Carrington M. 2013. Influence of HLA-C expression level on HIV control. Science 340:87–91. http://dx.doi.org/10.1126/science.1232685.

Immunity
Article

A Molecular Basis for the Control of Preimmune Escape Variants by HIV-Specific CD8$^+$ T Cells

Kristin Ladell,[1,11] Masao Hashimoto,[2,11] Maria Candela Iglesias,[3,11] Pascal G. Wilmann,[4,11] James E. McLaren,[1] Stéphanie Gras,[4] Takayuki Chikata,[2] Nozomi Kuse,[2] Solène Fastenackels,[3] Emma Gostick,[1] John S. Bridgeman,[1] Vanessa Venturi,[5] Zaïna Aït Arkoub,[6] Henri Agut,[6] David J. van Bockel,[7] Jorge R. Almeida,[3,8] Daniel C. Douek,[8] Laurence Meyer,[9] Alain Venet,[9] Masafumi Takiguchi,[2,12] Jamie Rossjohn,[1,4,12] David A. Price,[1,8,12] and Victor Appay[3,10,12,*]

[1]Institute of Infection and Immunity, Cardiff University School of Medicine, Heath Park, Cardiff CF14 4XN, Wales, UK
[2]Center for AIDS Research, Kumamoto University, 2-2-1 Honjo, Kumamoto 860-0811, Japan
[3]INSERM UMR S 945, Infections and Immunity, Université Pierre et Marie Curie-Paris6, Hôpital Pitié-Salpêtrière, 75013 Paris, France
[4]Department of Biochemistry and Molecular Biology, School of Biomedical Sciences, Monash University, Victoria 3800, Australia
[5]Computational Biology Group, Centre for Vascular Research, University of New South Wales, Kensington, Sydney, NSW 2052, Australia
[6]Virology Laboratory, ER1 DETIV UPMC, Université Pierre et Marie Curie-Paris6, Hôpital Pitié-Salpêtrière, 75013 Paris, France
[7]St Vincent's Centre for Applied Medical Research and University of New South Wales, Darlinghurst, Sydney, NSW 2010, Australia
[8]Human Immunology Section, Vaccine Research Center, National Institute of Allergy and Infectious Diseases, National Institutes of Health, Bethesda, MD 20892, USA
[9]INSERM, Université Paris-Sud, Hôpital du Kremlin-Bicêtre, 94275 Le Kremlin-Bicêtre, France
[10]AP-HP, Groupe Hospitalier Pitié-Salpêtrière, Laboratoire d'Immunologie Cellulaire et Tissulaire, 75013 Paris, France
[11]These authors contributed equally to this work
[12]These authors contributed equally to this work
*Correspondence: victor.appay@upmc.fr
http://dx.doi.org/10.1016/j.immuni.2012.11.021

SUMMARY

The capacity of the immune system to adapt to rapidly evolving viruses is a primary feature of effective immunity, yet its molecular basis is unclear. Here, we investigated protective HIV-1-specific CD8$^+$ T cell responses directed against the immunodominant p24 Gag-derived epitope KK10 (KRWIILGLNK$_{263-272}$) presented by human leukocyte antigen (HLA)-B*2705. We found that cross-reactive CD8$^+$ T cell clonotypes were mobilized to counter the rapid emergence of HIV-1 variants that can directly affect T cell receptor (TCR) recognition. These newly recruited clonotypes expressed TCRs that engaged wild-type and mutant KK10 antigens with similar affinities and almost identical docking modes, thereby accounting for their antiviral efficacy in HLA-B*2705$^+$ individuals. A protective CD8$^+$ T cell repertoire therefore encompasses the capacity to control TCR-accessible mutations, ultimately driving the development of more complex viral escape variants that disrupt antigen presentation.

INTRODUCTION

Adaptive CD8$^+$ T cell immunity is critical for protection against viruses and other intracellular pathogens. At the molecular level, this host-pathogen conflict centers on T cell receptor (TCR) engagement of major histocompatibility complex class I (MHC-I) molecules bearing peptide fragments derived from the intracellular invader. The αβ TCR repertoire encompasses a phenomenal level of diversity, which is generated by somatic recombination of variable (V), diversity (D), and joining (J) gene segments, junctional modifications, and differential pairing of α and β chains. Theoretically, between 10^{15} and 10^{20} different TCRs can be generated by this process (Davis and Bjorkman, 1988; Lieber, 1991). However, because of size constraints and thymic selection, each individual harbors a repertoire estimated to contain around 2.5×10^7 TCRs (Arstila et al., 1999). The diversity of the peripheral TCR repertoire has profound implications for effective immune coverage (Nikolich-Zugich et al., 2004).

Rapidly evolving pathogens capable of intrahost evolution during the course of infection must contest with the array of TCRs available for deployment. This sets the stage for a "molecular arms race" between the pathogen and the host. Immune escape by mutation of targeted CD8$^+$ T cell epitopes is a cardinal feature of HIV-1 infection and represents a key obstacle to the successful development of an AIDS vaccine (Goulder and Watkins, 2004). Indeed, the intense antiviral pressure exerted by CD8$^+$ T cell responses drives the rapid selection of escape mutations from the earliest stages of infection (Goonetilleke et al., 2009). Eventually, the frequency of such mutations correlates with the prevalence of the restricting human leukocyte antigen (HLA) class I allele across the population as a whole (Dong et al., 2011; Kawashima et al., 2009; Moore et al., 2002). Nonetheless, certain HLA class I alleles, including HLA-B*27, can confer relative protection from disease progression (Kaslow et al., 1996). In HLA-B*27$^+$ individuals infected with HIV-1 clade B,

the immunodominant KK10 epitope ($KRWIILGLNK_{263-272}$) in p24 Gag is almost invariably targeted by $CD8^+$ T cells (Altfeld et al., 2006; Scherer et al., 2004). These KK10-specific $CD8^+$ T cells unleash potent effector functions (Almeida et al., 2007; Berger et al., 2011), and the conservation of this response is thought to account for the benefits conferred by HLA-B*27 expression.

A number of mutations in the KK10 epitope have been reported in HIV-1-infected patients. The commonly observed Leu268Met mutation was initially considered to be a compensatory change required for the later appearance of the Arg264Lys mutation, which is associated with increased viral loads and clinical progression (Ammaranond et al., 2011; Feeney et al., 2004; Goulder et al., 1997; Kelleher et al., 2001). However, we recently showed that the Leu268Met mutation enables HIV-1 to evade recognition by highly effective $CD8^+$ T cells, including clonotypes defined by the expression of public TRBV4-3 TRBJ1-3 TCRs, which can be shared between individuals responding to the KK10 epitope (Iglesias et al., 2011). Nonetheless, control of viral replication is usually preserved despite this mutation. In HIV-1-infected patients presenting primarily a Leu268Met virus, the KK10-specific $CD8^+$ T cell response seems to be more reactive against the Leu268Met variant compared to the wild-type (WT) epitope; the converse applies in patients presenting a predominant WT virus (Iglesias et al., 2011; Lichterfeld et al., 2007; Streeck et al., 2008). These observations suggest that the immune response can adapt to mutations within the KK10 peptide that remain accessible to the TCR repertoire. However, the precise mechanism responsible for the maintenance of immune control in this situation remains unclear. Here, we show that the immune system can counter the emergence of Leu268Met variants through the mobilization of newly generated cross-reactive KK10-specific $CD8^+$ T cells, in particular those bearing TRBV6-5 TRBJ1-1 TCRs. These clonotypes were able to control both WT and Leu268Met viruses and retained potent suppressive capacity unless the virus succeeded in acquiring mutations, such as Arg264Lys, that negatively impact epitope presentation.

RESULTS

Emergence of Cross-Reactive WT and Leu268Met KK10-Specific $CD8^+$ T Cells during Primary HIV-1 Infection

To understand how KK10-specific $CD8^+$ T cell populations adjust to the early emergence of the Leu268Met mutant and maintain control of viral replication, we examined the fine specificity of responses to this epitope in HLA-B*2705$^+$ patients with primary HIV-1 infection. For this purpose, WT, Leu268Met, or dually reactive KK10-specific $CD8^+$ T cells were identified directly ex vivo by flow cytometry with fluorescent HLA-B*2705-peptide tetramers (Figure 1A). During early infection (i.e., within 3 months of viral transmission), robust $CD8^+$ T cell responses against WT, but not Leu268Met, KK10 could be detected in three patients (Figures 1A and 1B). These $CD8^+$ T cell populations engaged WT KK10 antigen (Ag) with high avidity, as revealed by staining with the corresponding CD8-null tetramer. Previous studies have shown that this physical parameter correlates with potent HIV-suppressive capacity (Almeida et al., 2007, 2009; Berger et al., 2011). Subsequently, we observed $CD8^+$ T cell expansions with reactivity against the Leu268Met variant (Figures 1A and 1B). These distinct populations exhibited high avidities for the cognate Ag in two patients (PrInf A and B) with stable control of viral replication in the absence of antiretroviral therapy. In contrast, lower-avidity Leu268Met KK10-specific $CD8^+$ T cells were present in patient PrInf C, who initiated antiretroviral therapy 18 months after infection as a result of progressively increasing viral loads (Figure 1C).

Extensive viral sequencing, from both plasma and peripheral blood mononuclear cells, was conducted to inform the observed patterns of KK10 reactivity (Figure 1C and Table S1 available online). In PrInf C, expansion of the Leu268Met KK10-specific $CD8^+$ T cell population coincided with the emergence of detectable Leu268Met variant virus at month 18. Indeed, the Leu268Met sequence was dominant at the cell-associated DNA level, indicating that the corresponding variant virus was poorly controlled in this patient. In patients PrInf A and B, however, the high-avidity Leu268Met KK10-specific $CD8^+$ T cell populations expanded without evidence of the Leu268Met mutation. Indeed, the Leu268Met sequence was detected in the cell-associated DNA from PrInf A only at a very late time point, after the initiation of antiretroviral therapy. Collectively, these data indicate that the immune system can generate high-avidity cross-reactive WT and Leu268Met KK10-specific $CD8^+$ T cells soon after primary HIV-1 infection, even with frequencies of Leu268Met variant virus that lie below the limit of detection with conventional sequencing methodologies.

High-Avidity WT and Leu268Met KK10-Specific $CD8^+$ T Cells Incorporate TRBV6-5 TRBJ1-1 Motif-Bearing TCRs

To characterize the molecular basis for WT and Leu268Met cross-reactivity at the level of TCR usage, we performed ex vivo analyses of *TRB* gene expression in both WT and dually reactive WT and Leu268Met KK10-specific $CD8^+$ T cell populations (Figure 2). $CD8^+$ T cell populations specific for the WT epitope were characterized by the turnover of recurrent clonotypes, several of which used the *TRBV4-3* gene as described previously (Iglesias et al., 2011). In contrast, the WT and Leu268Met KK10-specific $CD8^+$ T cell populations comprised entirely distinct clonotypes, suggesting de novo mobilization from the naive pool. The high-avidity WT and Leu268Met KK10-specific $CD8^+$ T cells observed in patients PrInf A and PrInf B showed particular enrichments for TRBV6-5 TRBJ1-1 clonotypes. Furthermore, TRBV6-5 TRBJ1-1 clonotypes were detected in both WT and Leu268Met KK10-specific $CD8^+$ T cell populations in two untreated HLA-B*2705$^+$ patients during the chronic phase of HIV infection (ChInf D and E; Figure S1A). The CDR3β sequence differed by a maximum of three amino acids between these TCRs (Figure 1D), indicating that a TRBV6-5 TRBJ1-1 motif (CASRXGXGXTEAF) can underpin WT and Leu268Met cross-reactivity. Of note, a similar CDR3β sequence was recently detected in an HIV-1-infected patient with elite control of viral replication (Chen et al., 2012). Molecular analysis of *TRA* gene expression revealed that the TRBV6-5 TRBJ1-1 clonotypes were accompanied by TRAV14 TRAJ21 transcripts in the respective $CD8^+$ T cell populations from PrInf

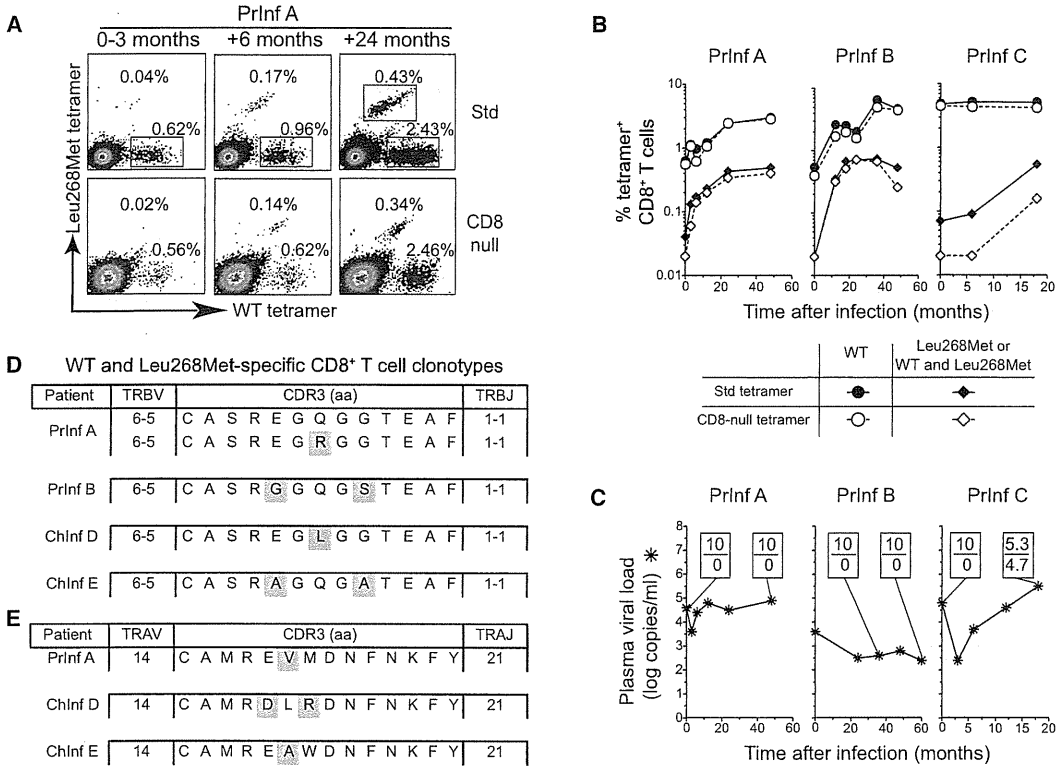

Figure 1. Ex Vivo Analysis of WT and Leu268Met KK10-Specific CD8+ T Cells

(A) Simultaneous WT and Leu268Met HLA-B*2705-KK10 tetramer staining of PBMCs from one HIV-1-infected patient (PrInf A) during and after primary infection. CD8+ T cells were stained with standard (Std) tetramers (top) and CD8-null tetramers (bottom); the latter selectively identify high-avidity cells. The percentages and flow cytometric sorting gates for WT versus Leu268Met or WT and Leu268Met KK10-specific tetramer+CD8+ T cell populations are shown.

(B) Kinetics of WT versus Leu268Met or WT and Leu268Met KK10-specific CD8+ T cell expansions in three patients (PrInf A, B, and C) from primary HIV-1 infection onward. Standard and CD8-null tetramer+CD8+ T cells are shown.

(C) Plasma viral load measurements in three patients (PrInf A, B, and C) from primary HIV-1 infection onward. The Leu268/Met268 ratio within the KK10 epitope is shown at two time points based on viral sequencing from plasma or cell-associated DNA.

(D) CDR3β amino acid sequence of TRBV6-5 TRBJ1-1 clonotypes within WT and Leu268Met KK10-specific CD8+ T cell populations from four HIV-1-infected patients: PrInf A and B (24 and 18 months after primary infection, respectively) and ChInf D and E (chronic infection).

(E) CDR3α amino acid sequence of TRAV14 TRAJ21 transcripts within WT and Leu268Met KK10-specific CD8+ T cell populations from three HIV-1-infected patients: PrInf A (24 months after primary infection) and ChInf D and E (chronic infection).

See also Table S1.

A and ChInf D (Figures 1E and S1B). Moreover, a subdominant TRAV14 TRAJ21 sequence was detected in the Leu268Met KK10-specific CD8+ T cell population in ChInf E. These data support a preferential pairing of TRBV6-5 TRBJ1-1 and TRAV14 TRAJ21 chains in KK10-specific CD8+ T cell clonotypes.

TRBV6-5 TRBJ1-1 Clonotypes Control WT and Leu268Met Viruses Effectively

To evaluate the functional impact of WT and Leu268Met cross-reactivity in more detail, we generated a CD8+ T cell clone (C12C) bearing a TRBV6-5 TRBJ1-1 TRAV14 TRAJ21 TCR (Figure 3A). The functional properties of C12C were evaluated in parallel with two other clones, one with high avidity specifically for the WT KK10 epitope (E2C) and one with low avidity for the same Ag (H8B); the latter clone was included to illustrate poor CD8+ T cell efficacy in our assays (Iglesias et al., 2011). Both WT and Leu268Met HLA-B*2705-KK10 tetramers costained C12C, in contrast to E2C and H8B. Moreover, C12C stained with the corresponding CD8-null tetramers, indicating high levels of avidity for both the WT and Leu268Met epitopes (Figure 3B). This highly avid dual recognition was reflected functionally in cytolytic Cr^{51} release assays, with C12C demonstrating sensitive responses to both forms of the epitope in peptide titrations (Figure 3C). To expand these findings, we measured degranulation (CD107a mobilization) and the intracellular production of IFN-γ, TNF-α, IL-2, and MIP-1β by these clones in response to primary HLA-B*2705+ CD4+ T cells infected with HIV_{NL4-3} viruses expressing either the WT or Leu268Met forms of the KK10 epitope (Figure 3D). In addition, we assessed the elimination of HIV-infected primary HLA-B*2705+ CD4+ target cells in vitro (Figure 3E). In line with the previous results, C12C displayed a robust polyfunctional profile in the presence of either WT or Leu268Met viruses and efficiently suppressed the replication of both HIV strains in primary CD4+ T cells. These features have all been

Patient PrInf A

0-3 months

WT KK10

TRBV	CDR3	TRBJ	Freq (%)	Count	
7-8	CASSSSSQEQF	2-1	39.77	35	
7-8	CASSLEPGTSSYNEQF	2-1	26.14	23	
20-1	CSARDINPGLAYEQY	2-1	13.64	12	
6-2/6-3	CASSPDSNNEQF	2-1	6.82	6	
4-3	CASSQGLQGSEQF	2-1	5.68	5	
5-1	CASSFVDSLSNQPQH	1-5	3.41	3	
9	CASSLHRDTEAF	1-1	3.41	3	
7-8	CASSLEPGTNSYNEQF	2-1	1.14	1	

+3 months

WT KK10

TRBV	CDR3	TRBJ	Freq (%)	Count	
28	CASGDRQNSPLH	1-6	58.70	54	
7-8	CASSSSSQEQF	2-1	26.09	24	
6-5	CASRGTSGTIEQF	2-1	3.26	3	
7-9	CASSLDRNEQF	2-1	3.26	3	*
5-1	CASSFVDSLSNQPQH	1-5	2.17	2	
4-3	CASSQGMFDYGYT	1-2	2.17	2	
12-3/12-4	CASSPTSGIEETQY	2-5	2.17	2	
7-9	CASNLDRNEQF	2-1	1.09	1	
7-8	CANSSSSQEQF	2-1	1.09	1	

+6 months

WT KK10

TRBV	CDR3	TRBJ	Freq (%)	Count
5-1	CASSLRGLAFTSSYNEQF	2-1	31.87	29
4-3	CASSQGQFGNEQF	2-1	28.57	26
7-9	CASSHGDYEQY	2-7	20.88	19
12-3/12-4	CASKKSTGGNTDTQY	2-3	12.09	11
9	CASSVDRDTEAF	1-1	4.40	4
5-1	CASSLRGLASTSSYNEQF	2-1	1.10	1
5-1	CASSLRGLAFSYSYNEQF	2-1	1.10	1

+12 months

WT KK10

TRBV	CDR3	TRBJ	Freq (%)	Count
5-1	CASSFVDSLSNQPQH	1-5	25.88	22
28	CASSSRQNTEAF	1-1	14.12	12
28	CASSDRQNTEAF	1-1	12.94	11
27	CASSHRTGELF	2-2	11.76	10
28	CASGDRQNSPLH	1-6	10.59	9
4-3	CASSQGQFGNEQF	2-1	7.06	6
4-3	CASSSGLAGGREQY	2-7	4.71	4
4-3	CASSQGMFDYGYT	1-2	3.53	3
7-8	CASSSSSQEQF	2-1	3.53	3
4-3	CASSQGLLASLEQY	2-7	2.35	2
10-2	CASRRGGLEIEQY	2-7	2.35	2
28	CAGSSRQNTEAF	1-1	1.18	1

+24 months

WT KK10

TRBV	CDR3	TRBJ	Freq (%)	Count	
28	CASGDRQNSPLH	1-6	45.33	34	
4-3	CASSQGQFGNEQF	2-1	14.67	11	
4-3	CASSPGQYSHEQY	2-7	12.00	9	
27	CASSRNNIEAF	1-1	5.33	4	
29-1	CSVPEQF	2-1	5.33	4	
5-1	CASSFVDSLSNQPQH	1-5	2.67	2	
5-5	CASSLRLLLYEQY	2-7	2.67	2	
27	CATSGITGELF	2-2	2.67	2	
5-1	CASSLRGIQTDSYNEQF	2-1	1.33	1	
5-1	CASSLRGIQTDSHNEQF	2-1	1.33	1	
28	CASSPGTGGDYGYT	1-2	1.33	1	
4-3	CGSSPGQYSHEQY	2-7	1.33	1	
4-3	CVSSQGQFGNEQF	2-1	1.33	1	
28	CASSSRQNTEAF	1-1	1.33	1	#
27	CATSGITRELF	2-2	1.33	1	

+24 months

Leu268Met or WT and Leu268Met

TRBV	CDR3	TRBJ	Freq (%)	Count
6-5	CASREGQGGTEAF	1-1	51.52	34
4-3	CASSLGTSSSYEQY	2-7	28.79	19
6-2	CASTLGTKRF	2-1	16.67	11
6-5	CASREGRGGTEAF	1-1	1.52	1
6-2	CARTLGTKRF	2-1	1.52	1

Patient PrInf B

0-3 months

WT KK10

TRBV	CDR3	TRBJ	Freq (%)	Count	
6-1	CASSSQENTEAF	1-1	57.1	20	
28	CASSDRQNSPLHF	1-6	31.4	11	
7-9	CASSLDRNEQF	2-1	5.7	2	*
5-1	CASSLDPPAGVSPLHF	1-6	2.9	1	
28	CASSSRQNTEAF	1-1	2.9	1	#

+18 months

WT KK10

TRBV	CDR3	TRBJ	Freq (%)	Count	
4-3	CASSQGQLNTQYF	2-3	36.8	25	
7-9	CASSLGEQPQHF	1-5	35.3	24	
28	CASSSRQNTEAF	1-1	7.4	5	#
28	CASSTRQNTEAF	1-1	7.4	5	
4-3	CASSQGRRSIEQF	2-1	4.4	3	
27	CASSSRTGELF	2-2	4.4	3	+
4-3	CASSPGVLGNTIYF	1-3	2.9	2	
28	CASSTRQNAEAF	1-1	1.5	1	

+18 months

Leu268Met or WT and Leu268Met

TRBV	CDR3	TRBJ	Freq (%)	Count
6-5	CASRGGQGSTEAF	1-1	100.0	65

Patient PrInf C

0-3 months

WT KK10

TRBV	CDR3	TRBJ	Freq (%)	Count	
7-9	CASSPYSGSYEQY	2-7	16.46	13	
12-5	CASGLGPSGTEAF	1-1	12.66	10	
20-1	CSARTLEGILTTGETQY	2-5	11.39	9	
27	CASSPRTGELF	2-2	10.13	8	
4-3	CASSLGTSAYEQY	2-7	8.86	7	
25-1	CTRAYNQPQH	1-5	6.33	5	
11-2	CASTIPPGTSVSGELF	2-2	5.06	4	
21-1	CASSKCRDKSYEQY	2-7	2.53	2	
4-3	CASGSGLANNEQF	2-1	2.53	2	
25-1	CASSEGNTGELF	2-2	2.53	2	
27	CASSRHTGELF	2-2	2.53	2	
27	CASRPSNTEAF	1-1	2.53	2	
7-9	CASSLDRNEQY	2-7	2.53	2	
20-1	CSARTLEGILTTGEAQY	2-5	1.27	1	
11-2	CASTIPPRTSVSGELF	2-2	1.27	1	
4-3	CASSPGLATDNEQF	2-1	1.27	1	
9	CASSRADLSYEQY	2-7	1.27	1	
6-5	CASSPGAYGNTIY	1-3	1.27	1	
4-3	CASSLGTSANEQF	2-7	1.27	1	
4-3	CASSQGRRSNEQF	2-1	1.27	1	
27	CASSSRTGELF	2-2	1.27	1	+
27	CASSRRTGELF	2-2	1.27	1	
27	CASSQRTGELF	2-2	1.27	1	
7-9	CASSFDSYEQY	2-7	1.27	1	

+6 months

WT KK10

TRBV	CDR3	TRBJ	Freq (%)	Count
7-9	CASSPYSGSYEQY	2-7	8.33	6
7-9	CASSPRSLSYEQY	2-7	8.33	6
4-3	CASSQGTSDYEQY	2-7	8.33	6
27	CASSQRTGELF	2-2	8.33	6
27	CASSGNTGELF	2-2	6.94	5
7-9	CASSFDSYEQY	2-7	5.56	4
20-1	CSARTLEGILTTGETQY	2-5	4.17	3
11-2	CASTIPPGTSVSGELF	2-2	2.78	2
21-1	CASSKCRGKSYEQY	2-7	2.78	2
4-3	CASGSGLANNEQF	2-1	2.78	2
27	CASSYRTGELF	2-2	2.78	2
27	CASSRSTGELF	2-2	2.78	2
7-9	CASSYDRNEQF	2-1	2.78	2
23-1	CASSHLDSPISNQPQH	1-5	1.39	1
7-9	CASSLGQQISGNTMY	1-3	1.39	1
4-1	CASSQDVLAGRREQY	2-7	1.39	1
29-1	CSVEGGTSGSYEQY	2-7	1.39	1
28	CASSLLGGDLYEQY	2-7	1.39	1
4-3	CASSQGTSDLYEQY	2-7	1.39	1
4-3	CASSLGTSDLYEQY	2-7	1.39	1
9	CASSVADLSYEQY	2-7	1.39	1
9	CASSRADLSYEQY	2-7	1.39	1
7-9	CASSPYSGSYEQF	2-7	1.39	1
4-3	CASSQGVAGAEQY	2-7	1.39	1
4-3	CASSPGTSAYEQY	2-7	1.39	1
4-3	CASSPGLSGNTIY	1-3	1.39	1
28	CASSSLDTGELF	2-2	1.39	1
28	CASSPGDGQPQH	1-5	1.39	1
27	CASSGTLEGGYT	1-2	1.39	1
25-1	CASSEGNTGELF	2-2	1.39	1
7-7	CASSFGQGYEQF	2-1	1.39	1
27	CASSRRTGELF	2-2	1.39	1
27	CASSRHTGELF	2-2	1.39	1
27	CASSGTTGELF	2-2	1.39	1
20-1	CSARTSDFEQF	2-1	1.39	1
7-9	CASSTYDRDEQY	2-7	1.39	1
7-9	CASSLDRGDQY	1-5	1.39	1

+18 months

WT KK10

TRBV	CDR3	TRBJ	Freq (%)	Count
27	CASSYRTGELF	2-2	30.00	21
20-1	CSARTLEGILTTGETQY	2-5	12.86	9
9	CASSRADLSYEQY	2-7	10.00	7
4-3	CASSQGLAGREQY	2-7	7.14	5
24-1	CATSDVNGAYEQY	2-7	5.71	4
4-3	CASGSGLANNEQF	2-1	5.71	4
5-1	CASSAESTRLTDTQY	2-3	4.29	3
4-3	CASSQGTSDLYEQY	2-7	4.29	3
7-9	CASSLDRNEQY	2-7	4.29	3
23-1	CASSHLDSPISNQPQH	1-5	2.86	2
4-3	CASSQGTSDYEQY	2-7	2.86	2
4-3	CASSLGQRSTEAF	1-1	2.86	2
7-8	CASSSYRGGGTEAF	1-1	1.43	1
9	CASSRADDSYEQY	2-7	1.43	1
4-3	CASSQGTSDYGQY	2-7	1.43	1
27	CASSYGTGELF	2-2	1.43	1
7-9	CASSYDRNEQF	2-1	1.43	1

+18 months

Leu268Met or WT and Leu268Met

TRBV	CDR3	TRBJ	Freq (%)	Count
20-1	CSARGGSVFYEQY	2-7	48.86	43
20-1	CSARGGERFYEQY	2-7	15.91	14
9	CASSASTSDYSYEQY	2-7	12.50	11
25-1	CASSDLTGTAYNEQF	2-1	11.36	10
20-1	CSDRGGSVFYEQY	2-7	2.27	2
20-1	CSARGGEGFYEQY	2-7	2.27	2
20-1	CSARGGAVFYEQY	2-7	2.27	2
25-1	CASSDLTGTVYNEQF	2-1	1.14	1
20-1	CSAWGGSVFYEQY	2-7	1.14	1
20-1	CSARGRERFYEQY	2-7	1.14	1
4-3	CASSPGVADTQY	2-3	1.14	1

(legend on next page)

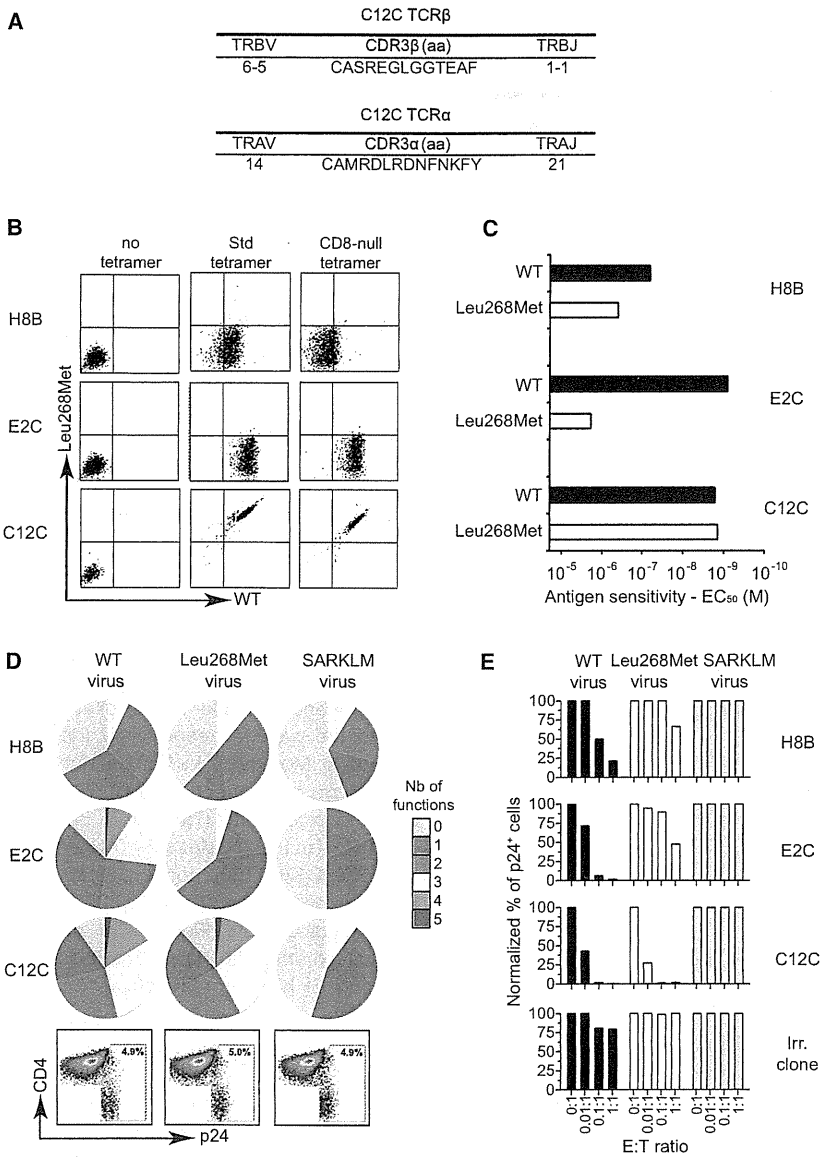

Figure 3. Functional Characterization of the CD8+ T Cell Clone C12C

(A) TCRβ and TCRα amino acid sequences of the C12C clone. This clone was derived from patient ChInf D (Figure S1).

(B) Comparative stainings of three KK10-specific CD8+ T cell clones (H8B, E2C, and C12C) with WT or Leu268Met HLA-B*2705-KK10 tetramers (standard or CD8 null). A pretitrated concentration of each tetramer (0.1 μg/ml) was used to highlight interclonal avidity differences.

(C) Antigen sensitivities (i.e., EC_{50} values in Cr^{51} release assays) of the KK10-specific CD8+ T cell clones H8B, E2C, and C12C.

(D) Polyfunctional profiles of H8B, E2C, and C12C after incubation for 6 hr with primary HLA-B*2705+CD4+ T cells infected with HIV_{NL4-3} viruses expressing either WT, Leu268Met, or the compound Ser173Ala+Arg264Lys+Leu268Met (SARKLM) mutation (CD8:CD4 ratio 10:1). The pie charts depict the background-adjusted polyfunctional profile of the CD8+ T cell clones. For simplicity, responses are grouped according to the number of functions elicited upon antigen encounter; individual segments represent the proportions of cells within each total clonal population that exhibited the number of functions indicated. The following functions were assessed: CD107a, IFN-γ, TNF-α, IL-2, and MIP-1β. In the bottom panel, representative stainings of primary CD4+ T cells at day 3 postinfection with WT, Leu268Met, or SARKLM HIV_{NL4-3} viruses are shown to demonstrate that infection rates (intracellular p24 expression) were equivalent in these experiments.

(E) Suppression of HIV replication in primary HLA-B*2705+CD4+ T cells infected with WT (black bars), Leu268Met (white bars), or SARKLM (gray bars) HIV_{NL4-3} viruses by H8B, E2C, and C12C at different E:T ratios. An irrelevant clone (Irr.) with specificity for an epitope derived from cytomegalovirus is shown as a negative control. The percentage of p24+CD4+ T cells was measured by flow cytometry at day 3 postinfection.

Representative data from three independent experiments are shown.

linked with CD8+ T cell efficacy against HIV in vivo (Appay et al., 2008).

Next, we assessed the impact of C12C on viral selection in vitro. For this purpose, we cocultured target cells infected with both "primary" and "emerging" viruses (e.g., WT and Leu268Met HIV_{NL4-3} strains) together with CD8+ T cell clones, then sequenced the residual viral population (Figure S2). Ratios of WT versus mutant virus were determined according to relative peak height on the sequencing electrogram; this approach was adapted to detect frequencies as low as 10% of the total viral population. Although the suppressive capacity of E2C was evident in this assay (Figure 4A), the presence of this clone resulted in selection of the Leu268Met mutant over the WT virus (Figure 4C), consistent with the inability of E2C to recognize the Leu268Met epitope. In contrast, H8B did not select for the Leu268Met mutant because of its low avidity and poor HIV-suppressive capacity (Figures 4A and 4C). Importantly, C12C suppressed HIV replication efficiently in this assay without selecting for the Leu268Met mutant. These results support our previous observations in vivo that CD8+ T cells with high levels

Figure 2. Clonotype Usage in KK10-Specific CD8+ T Cell Populations from Primary HIV-1 Infection Onward

TRBV and TRBJ usage, CDR3β amino acid sequence, and clonotype frequency are shown for WT and Leu268Met or dually reactive KK10-specific tetramer+CD8+ T cell populations isolated directly ex vivo from three patients (PrInf A, B, and C) during and after primary HIV-1 infection. Representative flow cytometric sorting gates are shown in Figure 1A. Recurrent clonotypes across time points within patients are color coded. Symbols denote public clonotypes within this data set. See also Figure S1.

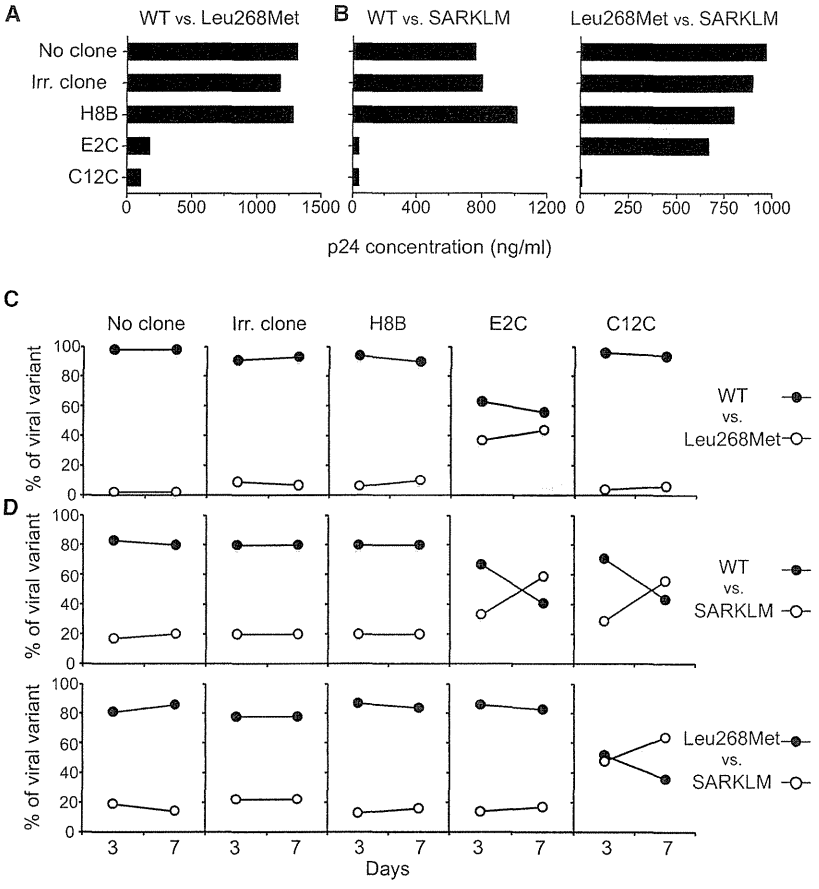

Figure 4. Impact of Distinct CD8+ T Cell Recognition Properties on Viral Selection In Vitro

(A and B) p24 concentrations at day 7 postinfection of 721.221-CD4-B*2705 cells with WT and Leu268Met (A), WT and SARKLM, or Leu268Met and SARKLM (B) viruses in the presence of the indicated CD8+ T cell clones.

(C and D) In vitro selection of viral mutants by KK10-specific CD8+ T cell clones. Percentages of WT and Leu268Met (C), WT and SARKLM, or Leu268Met and SARKLM (D) viruses were determined at day 3 and day 7 postinfection of 721.221-CD4-B*2705 cells cocultured in the presence of the indicated CD8+ T cell clones.

Representative data from two independent experiments are shown. See also Figure S2.

of sensitivity for the WT KK10 epitope in isolation can drive the emergence of early Leu268Met mutants (Iglesias et al., 2011). Collectively, these data indicate that the generation of CD8+ T cells bearing TCRs with dual reactivity can enable the immune system to counter the emergence of Leu268Met mutants.

HLA-B*2705 Recognition by a TRBV6-5 TRBJ1-1 Motif-Bearing TCR

To determine how TRBV6-5 TRBJ1-1 motif-bearing TCRs cross-recognize both the WT and Leu268Met epitopes, we expressed, refolded, and purified the C12C TCR. Surface plasmon resonance experiments showed that the C12C TCR bound both WT and Leu268Met forms of HLA-B*2705-KK10 with equivalent affinities (Kd ~1–5 μM) (Figure S3). This value falls at the high end of the affinity range previously determined for TCR interactions with MHC-I-peptide complexes (Bridgeman et al., 2012) and concurs with the observed tetramer binding and functional properties (Figure 3). Next, we determined the high-resolution crystal structures of the binary WT and Leu268Met HLA-B*2705-KK10 complexes and the corresponding ternary complexes with the C12C TCR (Table 1).

The binary structures showed that the KK10 epitope bound to HLA-B*2705 in a bulged and constrained conformation (Theodossis et al., 2010), with the flexible central part of the peptide protruding from the Ag-binding cleft (Figure 5A). The residues at P2, P3, P8, and P10 were buried in the Ag-binding cleft, whereas the residues at P1, P4–P7, and P9 were solvent exposed. The structure of the Leu268Met HLA-B*2705-KK10 epitope was virtually identical to that of the WT complex, with a root mean square deviation (rmsd) of 0.06 Å and 0.15 Å for the Ag-binding cleft and the peptide, respectively (data not shown). Moreover, the Leu268Met mutation did not affect HLA-B*2705-KK10 complex stability (Tm WT = 63.5°C ± 0.5°C, Tm Leu268Met = 64.0°C ± 1.0°C).

The C12C TCR docked at an angle of 57° across the WT HLA-B*2705-KK10 Ag-binding cleft (Figures 5B and 5C) and adopted a typical binding mode, with the Vα and Vβ domains positioned over the α2 and α1 helices, respectively (Burrows et al., 2010). Located toward the C-terminal end of the HLA-B*2705-KK10 Ag-binding cleft, the C12C TCR formed a total of 124 van der Waals (vdw) interactions and 16 hydrogen (H) bonds with a total buried surface area (BSA) at the interface of ~1,860 Å^2 (Table S2), comprising contributions of 58% and 42% from the Vα and Vβ domains, respectively. All six CDR loops of the C12C TCR contributed to the interaction with WT HLA-B*2705-KK10 (Figure 5C), albeit to varying degrees, with the predominant contacts being made via the CDR2α, CDR3α, and CDR3β loops (19.7%, 24.6%, and 19.8% of the BSA, respectively). Notably, the center of mass of the C12C TCR was shifted toward the α1 helix (77% of the HLA-B*2705 BSA), such that limited contacts were formed with the α2 helix (23% of the HLA-B*2705 BSA). Ligation-induced structural changes are described in Supplemental Information online (Figure S4).

The CDR2α loop was the only region of the C12C TCR that contacted the α2 helix of HLA-B*2705. Further, only two residues (Glu154 and Gln155) of the α2 helix of HLA-B*2705 were contacted by the C12C TCR, thereby representing the smallest contribution by the α2 helix seen in any TCR-MHC-I-peptide structure to date. In contrast, all six CDR loops of the C12C TCR contacted the α1 helix (Table S2). Arg62 was surrounded

Table 1. Data Collection and Refinement Statistics

Data Collection Statistics	C12C-HLA-B*2705^{KK10}	C12C-HLA-B*2705^{L268M}	HLA-B*2705^{KK10}	HLA-B*2705^{L268M}
Space group	$P2_1$	$P2_1$	$P2_12_12_1$	$P2_12_12_1$
Cell dimensions (Å, °)	56.68, 70.32, 107.77; β = 98.77	57.41, 71.31, 109.57; β = 98.80	51.21, 82.33, 109.24	51.27, 82.35, 109.60
Resolution (Å)	2.40 (2.53–2.40)	1.90 (2.00–1.90)	1.60 (1.69–1.60)	1.60 (1.69–1.60)
Total number of observations	243,277 (34,786)	255,452 (37,384)	438,464 (63,793)	409,890 (34,899)
Number of unique observations	32,993 (4,791)	68,882 (10,026)	61,797 (8,892)	55,998 (5,045)
Multiplicity	7.4 (7.3)	3.7 (3.7)	7.1 (7.2)	7.3 (6.9)
Data completeness (%)	100 (100)	99.8 (99.9)	100 (100)	90.5 (57.5)
I/σI	4.5 (1.8)	4.4 (1.6)	7.1 (2.8)	18.3 (4.8)
R_{pim} (%)[a]	5.9 (16.3)	7.0 (27.4)	6.9 (23.6)	2.6 (13.9)
Refinement Statistics				
Nonhydrogen Atoms				
Protein	6792	6884	3269	3277
Water	337	486	585	458
R_{factor} (%)[b]	17.8	18.6	19.7	19.1
R_{free} (%)[b]	25.7	24.5	23.7	22.7
Rms Deviation from Ideality				
Bond lengths (Å)	0.008	0.006	0.006	0.006
Bond angles (°)	1.128	1.022	0.987	1.038
Ramachandran Plot (%)				
Favored and allowed region	99.3	99.6	99.4	99.4
Generously allowed region	0.3	0.4	0.3	0.3
Disallowed region	0.4	0.0	0.3	0.3

Data collection and refinement statistics for the crystal structures of the binary WT and Leu268Met HLA-B*2705-KK10 complexes, as well as the corresponding ternary complexes with the C12C TCR, are indicated. Values in parentheses are for the highest-resolution shell.

[a] $R_{pim} = S_h [1(N-1)]^{1/2} Si|Ii(h) - <I(h)>| / ShSi Ii (h)$, where I is the observed intensity and <I> is the average intensity of multiple observations from symmetry-related reflections.

[b] $R_{factor} = Shkl ||Fo|-|Fc|| / Shkl |Fo|$ for all data except approximately 5%, which were used for R_{free} calculation.

by the CDR1α and CDR2α loops (Figure S5A), whereas the CDR3α loop contacted a more extensive region of the α1 helix (residues 62 to 69). The TCRβ chain contacted a focused region of the α1 helix (positions 72, 76, 79, and 83; Figure S5B). The interactions between the germline-encoded CDR1β and CDR2β loops were quite limited with respect to HLA-B*2705 binding (14.3% and 7.3% of the BSA, respectively), thereby suggesting that the biased *TRBV* gene usage was attributable to indirect mechanisms (Figure S6; Stadinski et al., 2011).

Viral Determinant Recognition by a TRBV6-5 TRBJ1-1 Motif-Bearing TCR

The WT KK10 peptide bulged centrally from the Ag-binding cleft and was contacted by the CDR1α, CDR2α, CDR3α, and CDR3β loops. Unlike the binary WT HLA-B*2705-KK10 structure, the entire region of the peptide was clearly resolved in the ternary complex, indicating that the conformation of the flexible peptide determinant was stabilized and altered by TCR ligation, as observed in other systems (Archbold et al., 2009; Tynan et al., 2007). The C12C TCR pivoted on the P6-Leu residue, and additionally contacted residues P1, P4–P5, P7, and P9, thereby ensuring broad coverage of the viral determinant. The CDR1α and CDR2α loops were positioned over the N-terminal region of the peptide contacting P1, P4, and P6, whereas the CDR3α loop was centrally located contacting P4 and P6, and the CDR3β loop was situated more toward the C-terminal end of the viral peptide contacting P6–P7 and P9 (Figure 5D). The P1-Lys residue was H-bonded to Gln30α, whereas the backbone of the CDR1α loop and Tyr59α from the CDR2α loop packed against the N-terminal "slope" of the peptide. The CDR3β loop was the only region of the TCRβ chain that interacted with the peptide, forming two H-bonds with P7-Gly and P9-Asn and a series of vdw interactions. The majority of these interactions involved Gly109β, Gly111β, and Thr113β, thereby providing structural explanations for both the CDR3β motif and preferential *TRBJ1-1* gene usage (Table S2). Importantly, P6-Leu was sequestered fully by the C12C TCR. The P6-Leu side chain protruded into a central, mostly hydrophobic, pocket that was enveloped by all three CDRα loops and the CDR3β loop and surrounded by a region of the CDR1α main chain, Phe113α, Tyr55α, Arg107α, Gly111β, and Thr113β. Thus, P6-Leu represented the central focal point of the C12C TCR.

The crystal structures of Leu268Met HLA-B*2705-KK10 in isolation and in complex with the C12C TCR showed how the P6-Leu-Met mutation was readily accommodated (Figure 5E). The density of the central region of the Leu268Met peptide was poorly defined in the binary structure, suggesting that the epitope was intrinsically flexible regardless of the amino acid at P6. The C12C TCR docked onto Leu268Met HLA-B*2705-KK10 in essentially an identical manner to that of the cognate

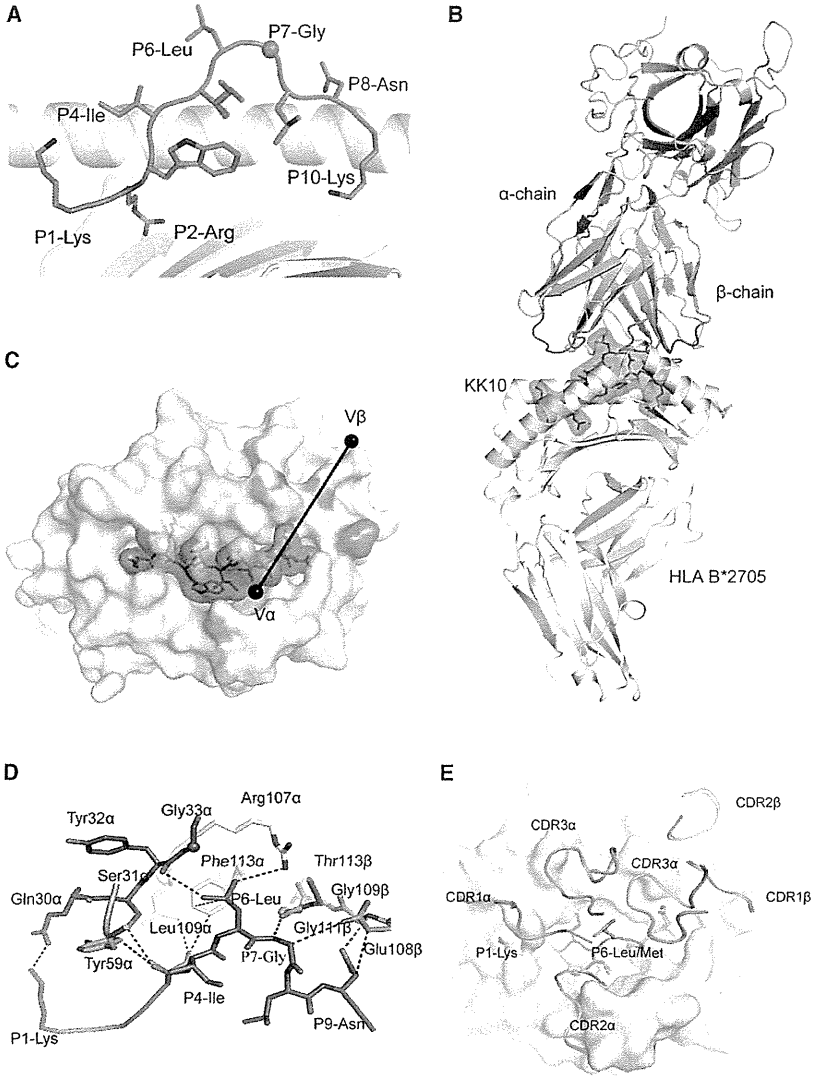

Figure 5. Structure of the C12C TCR in Complex with HLA-B*2705-KK10

(A) Cartoon representation of HLA-B*2705 with KK10 in stick representation. The sphere represents the Cα atom of P7-Gly.

(B) Cartoon representation of the C12C TCR in complex with HLA B*2705-KK10. The α chain of the C12C TCR is colored in pale pink, with the β chain in pale blue. The CDR1, 2, and 3 loops are colored in purple, green, and yellow for TCRα and blue, red, and orange for TCRβ, respectively. The HLA-B*2705 molecule is colored in white and the KK10 epitope is represented in pink stick and surface format.

(C) Footprint of the C12C TCR on the HLA-B*2705-KK10 surface, colored by CDR loop contact as in (B). The black spheres represent the center of mass for the Vα and Vβ domains of the C12C TCR.

(D) Interaction between the KK10 epitope (pink stick) and the C12C TCR loops. The spheres represent the Cα atoms of the glycine residues. The blue dashed lines represent vdw interactions and the red dashed lines represent hydrogen bonds.

(E) Superposition of the C12C TCR in complex with WT and Leu268Met HLA-B*2705-KK10. The peptides are represented in stick format and the CDR loops are shown in cartoon.

See also Figures S3–S6.

WT interaction (rmsd 0.39 Å), revealing that the mutation did not cause a significant repositioning of the C12C TCR (Figure 5E). Instead, P6-Met was located in the same pocket as P6-Leu and formed very similar interactions. Thus, the C12C TCR was perfectly adapted to cope with the P6-Leu-Met substitution, explaining the ability of the corresponding CD8+ T cell clone to cross-recognize both WT and Leu268Met KK10 epitopes and control the emergence of escape mutants.

TRBV6-5 TRBJ1-1 Motif-Bearing TCRs Are Not Readily Generated by Somatic Recombination

Each of the observed TRBV6-5 TRBJ1-1 clonotypes was encoded by only one nucleotide sequence. Analysis of these nucleotide sequences showed that the core of the CASRXGXGXTEAF motif was not predominantly germline encoded (Figure 6A). The two conserved glycines at CDR3β positions 5 and 7 could be completely attributed to the germline genes in only one of the five TRBV6-5 TRBJ1-1 clonotypes. For the other four clonotypes, only one of the two conserved glycines was completely germline encoded, and therefore nucleotide additions were necessary to generate amino acids in direct contact with the WT or Leu268Met peptide (Table S2). In contrast, multiple nucleotide sequences with predominant germline encoding of the associated motif have been observed both within and across individuals for TRBV4-3 TRBJ1-3 clonotypes, which are commonly mobilized and recognize only the WT form of the KK10 epitope with high avidity (Iglesias et al., 2011). Moreover, the TRBV6-5 TRBJ1-1 clonotypes required significantly higher numbers of nucleotide additions compared to the observed TRBV4-3 TRBJ1-3 clonotypes (Figure 6B). These observations suggested that production efficiency for the observed TRBV6-5 TRBJ1-1 clonotypes was relatively low, at least compared to the observed TRBV4-3 TRBJ1-3 TCRs. Thus, although the generation of KK10-specific CD8+ T cells bearing WT and Leu268Met cross-reactive TRBV6-5 TRBJ1-1 TCRs is an effective strategy to combat the appearance of Leu268Met variants, it may be challenging for the immune system to achieve this adaptation.

Eventual Viral Escape from Cross-Reactive WT and Leu268Met KK10-Specific CD8+ T Cells

Faced with TCR repertoire adaptation to viral variants, HIV has developed further means to escape KK10-specific CD8+ T cell recognition, namely the Arg264* mutation. Arg264Lys is the most frequently detected change, although Arg264Thr,

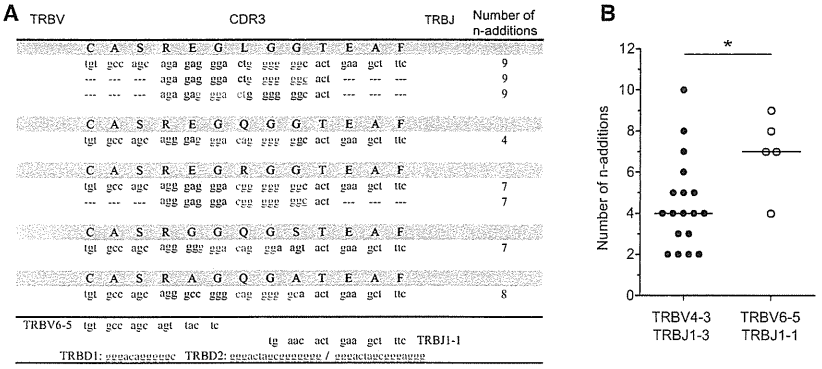

Figure 6. Genetic Coding of KK10-Specific TRBV6-5 TRBJ1-1 Clonotypes

(A) Shown are the observed nucleotide sequences coding for the TRBV6-5 TRBJ1-1 clonotypes described in this study, together with the contributions from the *TRBV* (green), *TRBD* (orange), and *TRBJ* (blue) genes that would require the minimum number of nucleotide additions (black). Potential P-additions are underlined. The multiple lines per nucleotide sequence display the multiple potential recombination events, i.e., different gene contributions and nucleotide additions, that could produce the observed nucleotide sequences with the minimum number of nucleotide additions.

(B) Comparative analysis of the minimal number of nucleotide additions required to generate the observed nucleotide sequences coding for TRBV6-5 TRBJ1-1 clonotypes versus TRBV4-3 TRBJ1-3 clonotypes. The TRBV4-3 TRBJ1-3 clonotypes considered in this analysis were those observed in this and previous studies (Iglesias et al., 2011). Statistical analysis was conducted the Mann-Whitney U-test. *$p < 0.05$.

Arg264Gln, and Arg264Gly substitutions have also been observed (Ammaranond et al., 2005; Betts et al., 2005; Feeney et al., 2004; Goulder et al., 2001; Kelleher et al., 2001; Pillay et al., 2005). The Arg264* mutation occurs at position 2 of the KK10 epitope, which acts as an anchor for HLA-B*27. Accordingly, the observed mutations at this position negatively affect epitope presentation via dramatic reductions in MHC-I-peptide binding affinity, which lead to decreased complex stability on the cell surface and impaired peptide loading during endogenous Ag processing (Ammaranond et al., 2005; Goulder et al., 1997, 2001). However, this mutation also impacts p24 structure and function; consequently, the Ser173Ala compensatory mutation is necessary to restore viral fitness (Schneidewind et al., 2007, 2008). The necessity for two discrete and simultaneous mutations represents a major constraint for the virus and has been proposed as an explanation for the late emergence of Arg264Lys mutants. Nonetheless, the eventual appearance of the Arg264Lys mutation abrogates the efficacy of KK10-specific $CD8^+$ T cells. None of the tested clones, including C12C, were able to suppress replication of a virus displaying the Ser173Ala, Arg264Lys, and Leu268Met mutations (SARKLM) (Figure 3E) or display polyfunctional profiles in the presence of primary HLA-B*2705$^+$ $CD4^+$ cells infected with SARKLM HIV_{NL4-3} (Figure 3D). Furthermore, although both C12C and E2C could drive the selection of the SARKLM mutant against WT virus in vitro, only the WT and Leu268Met cross-reactive clone C12C selected the SARKLM mutant against Leu268Met virus (Figures 4B and 4D). These data are consistent with the notion that SARKLM represents the ultimate escape virus and suggest that immune adaptation to Leu268Met, the early clonotype-specific escape mutant, drives the loss of KK10 binding to eliminate the possibility of further recognition by $CD8^+$ T cells.

DISCUSSION

Viral escape from $CD8^+$ T cell recognition is a hallmark of HIV-1 infection. The first escape variants can replace the original founder virus sequence within days and, as a consequence of ongoing immune pressure, sequential mutations follow (McMichael et al., 2010). Our data highlight the complex balance between viral evolution and immune adaptation focused on a single immunodominant epitope. In the context of HLA-B*2705, the early emergence of Leu268Met mutants is driven by high-avidity $CD8^+$ T cell clonotypes specific for the WT KK10 epitope (Iglesias et al., 2011). The Leu268Met substitution diminishes TCR recognition by these clonotypes, without cost to viral fitness. For HIV-1, this represents a rapid and effortless adaptation to host immunity. New KK10-specific $CD8^+$ T cell clonotypes endowed with WT and Leu268Met recognition capacity can then be recruited from the available repertoire. Indeed, previous studies have also observed changes in the KK10-specific $CD8^+$ T cell repertoire associated with the emergence of Leu268Met variants (Lichterfeld et al., 2007). This alternate clonotypic repertoire is readily able to control HIV-1 replication, as the appearance of the Leu268Met variant does not entail concomitant increases in plasma viremia (Ammaranond et al., 2011; Feeney et al., 2004; Goulder et al., 1997; Kelleher et al., 2001). Nonetheless, this clonotypic restructuring is probably not a trivial undertaking for an immune system already fundamentally compromised by the virus itself, in particular with respect to the loss of memory $CD4^+$ T cells and reduced naive T cell production (Appay and Sauce, 2008; Douek et al., 2009). In addition, WT and Leu268Met cross-reactive clonotypes can be relatively complex to generate. This feature may help to explain the diverse outcomes of HIV-1 infection across HLA-B*2705$^+$ cohorts, despite the overall protection associated with carriage of this allele and the almost universal immunodominance of the KK10 epitope (Goulder and Watkins, 2008). Eventually, though, the highly effective WT and Leu268Met KK10-specific $CD8^+$ T cell response drives the selection of new variants, in particular the Arg264Lys mutation. This new viral variant is more complex to produce because it requires the compensatory Ser173Ala mutation. However, because of the reduction in HLA-B*2705-KK10 peptide binding and presentation, this compound mutation renders the KK10-specific $CD8^+$ T cell response obsolete and therefore represents the ultimate viral adaptation in this system. Uncontrolled HIV-1 replication and disease progression ensue (Almeida et al., 2007; Ammaranond et al., 2011; Feeney et al., 2004; Goulder et al., 1997; Kelleher et al., 2001).

The present work illuminates the mechanism that underpins the control of HIV-1 replication in HLA-B*2705$^+$ individuals,

highlighting the importance of viral variant recognition by KK10-specific CD8+ T cell clonotypes (Chen et al., 2012). It seems likely that the dual specificity TRBV6-5 TRBJ1-1 clonotypes were selected from the available repertoire in response to the emergence of Leu268Met variants. Remarkably, the absence of detectable viral mutants in patients PrInf A and B suggests that such clonotypes may have been elicited by very low-frequency Leu268Met variants, which were subsequently suppressed effectively to the extent that they remained below the limit of detection with conventional subcloning and sequencing approaches. The functional properties of C12C were consistent with this possibility. In addition, a recent study has demonstrated the feasibility of this scenario in another system (Henn et al., 2012). Other clonotypes that recognize Leu268Met less sensitively, as observed in PrInf C, may well require higher frequencies of the variant to be mobilized and will suppress HIV-1 replication less effectively. The early prevalence of the Leu268Met variant in cell-associated DNA from PrInf C and the progressive loss of viral control observed in this patient are compatible with these speculations. Accordingly, the kinetics of the continuous competition between HIV-1 and CD8+ T cell-mediated adaptive immunity are probably critical determinants of viral control and pathogenesis.

Collectively, our findings suggest that the clonotypic nature of the responding CD8+ T cell repertoire and the subtle selection of TCRs conferring high-avidity recognition of both the WT and variant epitopes underpin viremic control and limit the emergence of escape mutations. Analysis of the C12C TCR in complex with HLA-B*2705-KK10 elucidated the molecular basis for effective dual recognition of the WT and Leu268Met epitopes by TRBV6-5 TRBJ1-1 motif-bearing TCRs. Of note, the CDR1β and CDR2β loop interactions were suboptimal with respect to HLA-B*2705 binding, suggesting that biased *TRBV6-5* gene usage may reflect preferred *TRBJ1-1* or *TRAV14* gene pairing. In keeping with this possibility, key residues involved in HLA-B*2705-KK10 binding were encoded only by the *TRAV14* gene. This is consistent with a recent study highlighting the influence of Vα pairing on Vβ recognition of the MHC-peptide complex (Stadinski et al., 2011). These considerations also align well with the observation that *TRAV14* gene usage has been associated with high-avidity WT KK10-specific CD8+ T cell clonotypes (Iglesias et al., 2011).

Other mutations at different positions within the KK10 epitope (e.g., 4, 5, 7, or 9) have been reported and might affect TCR recognition (Almeida et al., 2007; Ammaranond et al., 2011; Feeney et al., 2004; Goulder et al., 1997; Kelleher et al., 2001; van Bockel et al., 2011). These mutations are not associated with enhanced viral replication, suggesting that the capacity of the KK10-specific CD8+ T cell response to recruit cross-reactive clonotypes from the available repertoire is not limited to the Leu268Met variant. Indeed, the TRBV6-5 TRBJ1-1 clonotypes described herein probably represent an array of clonally distributed CD8+ T cells that fulfill the same protective role against HIV. This notion is supported by the observation of various dominant cross-reactive KK10-specific CD8+ T cell clonotypes in HLA-B*2705+ long-term nonprogressors or elite controllers (van Bockel et al., 2011; Chen et al., 2012). Such adaptation within the CD8+ T cell response probably impacts the durability of immune control and biological outcome. More generally, immune adaptation to TCR-accessible mutations may become limiting only in the case of highly restricted epitope-specific repertoires (Price et al., 2004). However, in the case of mutations that adversely impact MHC-I-peptide binding or Ag processing (Goulder and Watkins, 2004), or even lead to epitope deletion from the viral genome altogether (Price et al., 1997), the plasticity of the CD8+ T cell response becomes irrelevant. These considerations explain why the majority of described escape mutations in HIV-1 infection operate to minimize epitope presentation.

The present study provides unprecedented insights into the molecular arms race between HIV and CD8+ T cell immunity within a single epitope specificity. Although the enormity of such reciprocal adaptation across all potential epitopes is staggering, the data reported here illuminate the precarious nature of the incessant battle between host and virus that underlies the apparent equilibrium established during the chronic phase of HIV-1 infection.

EXPERIMENTAL PROCEDURES

Patients

Samples were obtained from asymptomatic HIV-1-infected HLA-B*2705+ patients enrolled in the French ANRS PRIMO cohorts. Antiretroviral therapy was initiated upon evidence of disease progression (i.e., persistent uncontrolled viral replication or CD4+ T cell counts < 500 cells/mm^3), occurring 6 years postinfection for PrInf A and B and 1.5 years postinfection for PrInf C. The study was approved by the Institutional Review Board and Local Ethics Committee of the Hôpital Pitié-Salpêtrière, Paris. Peripheral blood mononuclear cells (PBMCs) were separated from citrate anticoagulated blood and cryo-preserved for subsequent studies. Plasma and cell-associated HIV-1 *gag* sequencing was performed as described previously (Akahoshi et al., 2012).

Viruses and CD8+ T Cell Clones

HIV_{NL4-3} was modified to express one or more mutations in p24 Gag (Ser173Ala, Arg264Lys, and/or Leu268Met) via the GeneTailor site-directed mutagenesis system (Invitrogen) and oligonucleotide primers as described previously (Schneidewind et al., 2007). Viral stocks were generated by transfection of HEK293T cells with 30 μg of plasmid DNA. Supernatants were harvested 48 hr after transfection and frozen aliquots were stored at −80°C. The concentration of p24 Ag in viral stocks was measured by enzyme-linked immunosorbent assay (HIV-1 p24 Ag ELISA kit; ZeptoMetrix). HIV-specific CD8+ T cell clones were generated and maintained as described previously (Almeida et al., 2009). In brief, single HLA-B*2705-KK10 tetramer+CD8+ T cells were sorted by flow cytometry and expanded in microtiter plates by periodic stimulation in the presence of mixed irradiated allogeneic PBMCs, phytohemagglutinin (PHA; 1 μg/ml), and recombinant human IL-2 (rhIL-2; 150 IU/ml) in RPMI 1640 medium supplemented with 5% human AB serum, antibiotics, and L-glutamine.

Clonotype Analysis

Molecular analysis of *TRB* and *TRA* gene expression in KK10-specific tetramer+CD8+ T cell populations isolated directly ex vivo by flow cytometry was conducted via a template-switch anchored RT-PCR as described previously (Quigley et al., 2011). A similar approach was used to characterize *TRB* and *TRA* gene expression in KK10-specific CD8+ T cell clones. In all cases, TCR nomenclature was directly translated from the IMGT database by web-based alignment of molecular TRB or TRA transcripts (IMGT, The ImMunoGeneTics information system, http://www.imgt.org). The germline alignments for the TRBV6-5 TRBJ1-1 clonotypes were determined to allow for potential P-additions from the *TRBD* genes.

Functional Characterization of CD8+ T Cell Clones

Antigen sensitivity was assessed by measuring the peptide concentration required to induce half-maximal responses (EC_{50}) in cytolytic Cr^{51} release

assays with HLA-B*2705+ EBV-transformed B cell targets as described previously (Almeida et al., 2007, 2009). For functional profiling, CD8+ T cell clones were incubated for 1 hr at 37°C in the presence of αCD107a mAb and HLA-B*2705+CD4+ T cells infected 3 days earlier with titrated levels of WT or mutated HIV_{NL4-3} virus; monensin (2.5 μg/ml; Sigma-Aldrich) and brefeldin A (5 μg/ml; Sigma-Aldrich) were added for a further 5 hr. Staining for intracellular markers and data analysis were performed as described previously (Almeida et al., 2009). For HIV suppression assays, primary HLA-B*2705+ CD4+ T cells were purified from PBMCs by positive magnetic bead selection (Miltenyi Biotec), stimulated for 2 days with PHA (1 μg/ml), and cultured with 100 U/ml rhIL-2. Seven days later, 10^5 cells/well were infected with titrated levels of viruses by spinoculation (Iglesias et al., 2011) and mixed with CD8+ T cell clones at different CD8+/CD4+ ratios. Cells were harvested at day 3 postinfection, then stained for both CD4 and intracellular p24 to evaluate the elimination of HIV-infected targets. The protocol for competitive viral selection assays is provided in Supplemental Information online. Directly conjugated mAbs were purchased as follows: from BD Biosciences, αCD4-APCCy7, αCD107a-Cy5PE, αIL-2-APC, αIFNγ-Alexa700, and αTNFα-PECy7; from Caltag Laboratories, αCD8-Alexa405; from R&D Systems, αMIP-1β-FITC; and from Beckman Coulter, αp24-PE. The viability dye ViViD (Life Technologies) was used to eliminate dead cells from flow cytometric analyses.

Protein Production and Crystallography

Soluble recombinant proteins for structural and binding studies were produced as described previously with minor modifications (Gras et al., 2009; Iglesias et al., 2011; Price et al., 2005). Crystals of the C12C TCR in complex with WT and Leu268Met HLA-B*2705-KK10 were grown by the hanging-drop, vapor-diffusion method at 20°C with a protein reservoir drop ratio of 1:1 and a concentration of 5 mg/ml in 10 mM Tris (pH 8), 150 mM NaCl. Crystals grew in 24% PEG 3350 and 0.3 M Na_2SO_4. Crystals of the WT and Leu268-Met HLA-B*2705-KK10 complexes were grown by the same technique in a mother liquor containing 16% PEG 8000 and 0.1 M MES (pH 7.0). Data collection, processing, structure determination, refinement, and validation were conducted with standard crystallography software. Details are provided in Supplemental Information online.

Statistics

Group medians and distributions were compared by the Mann-Whitney U-test. p values less than 0.05 were considered significant.

ACCESSION NUMBERS

The atomic coordinates and structure factors were deposited in the Protein Data Bank with the following accession codes: 4G8G for the C12C TCR in complex with WT HLA-B*2705-KK10, 4G9F for the C12C TCR in complex with Leu268Met HLA-B*2705-KK10, 4G9D for WT HLA B*2705-KK10, and 4G8I for Leu268Met HLA B*2705-KK10.

SUPPLEMENTAL INFORMATION

Supplemental Information includes Supplemental Experimental Procedures, six figures, and two tables and can be found with this article online at http://dx.doi.org/10.1016/j.immuni.2012.11.021.

ACKNOWLEDGMENTS

We thank all study participants, the French Agence Nationale de la Recherche sur le SIDA (ANRS) Cohorts ALT and PRIMO groups, and the staff at the MX2 beamline (Australian synchrotron). We are grateful to C. Blanc for sorting viable infected cells at the Pitié-Salpêtrière Flow Cytometry Platform. This work was supported by the ANR (project ANR-09-JCJC-0114-01), Sidaction, the French ANRS, the National Institutes of Health via the Intramural Program of the Vaccine Research Center (National Institute of Allergy and Infectious Diseases), the Australian Research Council (ARC), the Australian National Health and Medical Research Council (NHMRC), the UK Biotechnology and Biological Sciences Research Council (grant BB/H001085/1), the Japanese Ministry of Health (grant 18390141), and the Global COE program ("Global Education and Research Center Aiming at the Control of AIDS") of the Japanese Ministry of Education, Science, Sports, and Culture. M.C.I. is supported by a Sidaction Fellowship. V.V. and S.G. are ARC Future Fellows. P.G.W. is an NHMRC CJ Martin Fellow. J.R. is an NHMRC Australia Fellow. D.A.P. is a Wellcome Trust Senior Investigator.

Received: March 24, 2012
Accepted: November 5, 2012
Published: March 21, 2013

REFERENCES

Akahoshi, T., Chikata, T., Tamura, Y., Gatanaga, H., Oka, S., and Takiguchi, M. (2012). Selection and accumulation of an HIV-1 escape mutant by three types of HIV-1-specific cytotoxic T lymphocytes recognizing wild-type and/or escape mutant epitopes. J. Virol. *86*, 1971–1981.

Almeida, J.R., Price, D.A., Papagno, L., Arkoub, Z.A., Sauce, D., Bornstein, E., Asher, T.E., Samri, A., Schnuriger, A., Theodorou, I., et al. (2007). Superior control of HIV-1 replication by CD8+ T cells is reflected by their avidity, polyfunctionality, and clonal turnover. J. Exp. Med. *204*, 2473–2485.

Almeida, J.R., Sauce, D., Price, D.A., Papagno, L., Shin, S.Y., Moris, A., Larsen, M., Pancino, G., Douek, D.C., Autran, B., et al. (2009). Antigen sensitivity is a major determinant of CD8+ T-cell polyfunctionality and HIV-suppressive activity. Blood *113*, 6351–6360.

Altfeld, M., Kalife, E.T., Qi, Y., Streeck, H., Lichterfeld, M., Johnston, M.N., Burgett, N., Swartz, M.E., Yang, A., Alter, G., et al. (2006). HLA alleles associated with delayed progression to AIDS contribute strongly to the initial CD8(+) T cell response against HIV-1. PLoS Med. *3*, e403.

Ammaranond, P., Zaunders, J., Satchell, C., van Bockel, D., Cooper, D.A., and Kelleher, A.D. (2005). A new variant cytotoxic T lymphocyte escape mutation in HLA-B27-positive individuals infected with HIV type 1. AIDS Res. Hum. Retroviruses *21*, 395–397.

Ammaranond, P., van Bockel, D.J., Petoumenos, K., McMurchie, M., Finlayson, R., Middleton, M.G., Davenport, M.P., Venturi, V., Suzuki, K., Gelgor, L., et al. (2011). HIV immune escape at an immunodominant epitope in HLA-B*27-positive individuals predicts viral load outcome. J. Immunol. *186*, 479–488.

Appay, V., and Sauce, D. (2008). Immune activation and inflammation in HIV-1 infection: causes and consequences. J. Pathol. *214*, 231–241.

Appay, V., Douek, D.C., and Price, D.A. (2008). CD8+ T cell efficacy in vaccination and disease. Nat. Med. *14*, 623–628.

Archbold, J.K., Macdonald, W.A., Gras, S., Ely, L.K., Miles, J.J., Bell, M.J., Brennan, R.M., Beddoe, T., Wilce, M.C., Clements, C.S., et al. (2009). Natural micropolymorphism in human leukocyte antigens provides a basis for genetic control of antigen recognition. J. Exp. Med. *206*, 209–219.

Arstila, T.P., Casrouge, A., Baron, V., Even, J., Kanellopoulos, J., and Kourilsky, P. (1999). A direct estimate of the human alphabeta T cell receptor diversity. Science *286*, 958–961.

Berger, C.T., Frahm, N., Price, D.A., Mothe, B., Ghebremichael, M., Hartman, K.L., Henry, L.M., Brenchley, J.M., Ruff, L.E., Venturi, V., et al. (2011). High-functional-avidity cytotoxic T lymphocyte responses to HLA-B-restricted Gag-derived epitopes associated with relative HIV control. J. Virol. *85*, 9334–9345.

Betts, M.R., Exley, B., Price, D.A., Bansal, A., Camacho, Z.T., Teaberry, V., West, S.M., Ambrozak, D.R., Tomaras, G., Roederer, M., et al. (2005). Characterization of functional and phenotypic changes in anti-Gag vaccine-induced T cell responses and their role in protection after HIV-1 infection. Proc. Natl. Acad. Sci. USA *102*, 4512–4517.

Bridgeman, J.S., Sewell, A.K., Miles, J.J., Price, D.A., and Cole, D.K. (2012). Structural and biophysical determinants of αβ T-cell antigen recognition. Immunology *135*, 9–18.

Burrows, S.R., Chen, Z., Archbold, J.K., Tynan, F.E., Beddoe, T., Kjer-Nielsen, L., Miles, J.J., Khanna, R., Moss, D.J., Liu, Y.C., et al. (2010). Hard wiring of T cell receptor specificity for the major histocompatibility complex is underpinned by TCR adaptability. Proc. Natl. Acad. Sci. USA *107*, 10608–10613.

Chen, H., Ndhlovu, Z.M., Liu, D., Porter, L.C., Fang, J.W., Darko, S., Brockman, M.A., Miura, T., Brumme, Z.L., Schneidewind, A., et al. (2012). TCR clonotypes modulate the protective effect of HLA class I molecules in HIV-1 infection. Nat. Immunol. *13*, 691–700.

Davis, M.M., and Bjorkman, P.J. (1988). T-cell antigen receptor genes and T-cell recognition. Nature *334*, 395–402.

Dong, T., Zhang, Y., Xu, K.Y., Yan, H., James, I., Peng, Y., Blais, M.E., Gaudieri, S., Chen, X., Lun, W., et al. (2011). Extensive HLA-driven viral diversity following a narrow-source HIV-1 outbreak in rural China. Blood *118*, 98–106.

Douek, D.C., Roederer, M., and Koup, R.A. (2009). Emerging concepts in the immunopathogenesis of AIDS. Annu. Rev. Med. *60*, 471–484.

Feeney, M.E., Tang, Y., Roosevelt, K.A., Leslie, A.J., McIntosh, K., Karthas, N., Walker, B.D., and Goulder, P.J. (2004). Immune escape precedes breakthrough human immunodeficiency virus type 1 viremia and broadening of the cytotoxic T-lymphocyte response in an HLA-B27-positive long-term-nonprogressing child. J. Virol. *78*, 8927–8930.

Goonetilleke, N., Liu, M.K., Salazar-Gonzalez, J.F., Ferrari, G., Giorgi, E., Ganusov, V.V., Keele, B.F., Learn, G.H., Turnbull, E.L., Salazar, M.G., et al.; CHAVI Clinical Core B. (2009). The first T cell response to transmitted/founder virus contributes to the control of acute viremia in HIV-1 infection. J. Exp. Med. *206*, 1253–1272.

Goulder, P.J., and Watkins, D.I. (2004). HIV and SIV CTL escape: implications for vaccine design. Nat. Rev. Immunol. *4*, 630–640.

Goulder, P.J., and Watkins, D.I. (2008). Impact of MHC class I diversity on immune control of immunodeficiency virus replication. Nat. Rev. Immunol. *8*, 619–630.

Goulder, P.J., Phillips, R.E., Colbert, R.A., McAdam, S., Ogg, G., Nowak, M.A., Giangrande, P., Luzzi, G., Morgan, B., Edwards, A., et al. (1997). Late escape from an immunodominant cytotoxic T-lymphocyte response associated with progression to AIDS. Nat. Med. *3*, 212–217.

Goulder, P.J., Brander, C., Tang, Y., Tremblay, C., Colbert, R.A., Addo, M.M., Rosenberg, E.S., Nguyen, T., Allen, R., Trocha, A., et al. (2001). Evolution and transmission of stable CTL escape mutations in HIV infection. Nature *412*, 334–338.

Gras, S., Burrows, S.R., Kjer-Nielsen, L., Clements, C.S., Liu, Y.C., Sullivan, L.C., Bell, M.J., Brooks, A.G., Purcell, A.W., McCluskey, J., and Rossjohn, J. (2009). The shaping of T cell receptor recognition by self-tolerance. Immunity *30*, 193–203.

Henn, M.R., Boutwell, C.L., Charlebois, P., Lennon, N.J., Power, K.A., Macalalad, A.R., Berlin, A.M., Malboeuf, C.M., Ryan, E.M., Gnerre, S., et al. (2012). Whole genome deep sequencing of HIV-1 reveals the impact of early minor variants upon immune recognition during acute infection. PLoS Pathog. *8*, e1002529.

Iglesias, M.C., Almeida, J.R., Fastenackels, S., van Bockel, D.J., Hashimoto, M., Venturi, V., Gostick, E., Urrutia, A., Wooldridge, L., Clement, M., et al. (2011). Escape from highly effective public CD8+ T-cell clonotypes by HIV. Blood *118*, 2138–2149.

Kaslow, R.A., Carrington, M., Apple, R., Park, L., Muñoz, A., Saah, A.J., Goedert, J.J., Winkler, C., O'Brien, S.J., Rinaldo, C., et al. (1996). Influence of combinations of human major histocompatibility complex genes on the course of HIV-1 infection. Nat. Med. *2*, 405–411.

Kawashima, Y., Pfafferott, K., Frater, J., Matthews, P., Payne, R., Addo, M., Gatanaga, H., Fujiwara, M., Hachiya, A., Koizumi, H., et al. (2009). Adaptation of HIV-1 to human leukocyte antigen class I. Nature *458*, 641–645.

Kelleher, A.D., Long, C., Holmes, E.C., Allen, R.L., Wilson, J., Conlon, C., Workman, C., Shaunak, S., Olson, K., Goulder, P., et al. (2001). Clustered mutations in HIV-1 gag are consistently required for escape from HLA-B27-restricted cytotoxic T lymphocyte responses. J. Exp. Med. *193*, 375–386.

Lichterfeld, M., Kavanagh, D.G., Williams, K.L., Moza, B., Mui, S.K., Miura, T., Sivamurthy, R., Allgaier, R., Pereyra, F., Trocha, A., et al. (2007). A viral CTL escape mutation leading to immunoglobulin-like transcript 4-mediated functional inhibition of myelomonocytic cells. J. Exp. Med. *204*, 2813–2824.

Lieber, M.R. (1991). Site-specific recombination in the immune system. FASEB J. *5*, 2934–2944.

McMichael, A.J., Borrow, P., Tomaras, G.D., Goonetilleke, N., and Haynes, B.F. (2010). The immune response during acute HIV-1 infection: clues for vaccine development. Nat. Rev. Immunol. *10*, 11–23.

Moore, C.B., John, M., James, I.R., Christiansen, F.T., Witt, C.S., and Mallal, S.A. (2002). Evidence of HIV-1 adaptation to HLA-restricted immune responses at a population level. Science *296*, 1439–1443.

Nikolich-Zugich, J., Slifka, M.K., and Messaoudi, I. (2004). The many important facets of T-cell repertoire diversity. Nat. Rev. Immunol. *4*, 123–132.

Pillay, T., Zhang, H.T., Drijfhout, J.W., Robinson, N., Brown, H., Khan, M., Moodley, J., Adhikari, M., Pfafferott, K., Feeney, M.E., et al. (2005). Unique acquisition of cytotoxic T-lymphocyte escape mutants in infant human immunodeficiency virus type 1 infection. J. Virol. *79*, 12100–12105.

Price, D.A., Goulder, P.J., Klenerman, P., Sewell, A.K., Easterbrook, P.J., Troop, M., Bangham, C.R., and Phillips, R.E. (1997). Positive selection of HIV-1 cytotoxic T lymphocyte escape variants during primary infection. Proc. Natl. Acad. Sci. USA *94*, 1890–1895.

Price, D.A., West, S.M., Betts, M.R., Ruff, L.E., Brenchley, J.M., Ambrozak, D.R., Edghill-Smith, Y., Kuroda, M.J., Bogdan, D., Kunstman, K., et al. (2004). T cell receptor recognition motifs govern immune escape patterns in acute SIV infection. Immunity *21*, 793–803.

Price, D.A., Brenchley, J.M., Ruff, L.E., Betts, M.R., Hill, B.J., Roederer, M., Koup, R.A., Migueles, S.A., Gostick, E., Wooldridge, L., et al. (2005). Avidity for antigen shapes clonal dominance in CD8+ T cell populations specific for persistent DNA viruses. J. Exp. Med. *202*, 1349–1361.

Quigley, M.F., Almeida, J.R., Price, D.A., and Douek, D.C. (2011). Unbiased molecular analysis of T cell receptor expression using template-switch anchored RT-PCR. Curr. Protoc. Immunol. *10*, 10.33.

Scherer, A., Frater, J., Oxenius, A., Agudelo, J., Price, D.A., Günthard, H.F., Barnardo, M., Perrin, L., Hirschel, B., Phillips, R.E., and McLean, A.R.; Swiss HIV Cohort Study. (2004). Quantifiable cytotoxic T lymphocyte responses and HLA-related risk of progression to AIDS. Proc. Natl. Acad. Sci. USA *101*, 12266–12270.

Schneidewind, A., Brockman, M.A., Yang, R., Adam, R.I., Li, B., Le Gall, S., Rinaldo, C.R., Craggs, S.L., Allgaier, R.L., Power, K.A., et al. (2007). Escape from the dominant HLA-B27-restricted cytotoxic T-lymphocyte response in Gag is associated with a dramatic reduction in human immunodeficiency virus type 1 replication. J. Virol. *81*, 12382–12393.

Schneidewind, A., Brockman, M.A., Sidney, J., Wang, Y.E., Chen, H., Suscovich, T.J., Li, B., Adam, R.I., Allgaier, R.L., Mothé, B.R., et al. (2008). Structural and functional constraints limit options for cytotoxic T-lymphocyte escape in the immunodominant HLA-B27-restricted epitope in human immunodeficiency virus type 1 capsid. J. Virol. *82*, 5594–5605.

Stadinski, B.D., Trenh, P., Smith, R.L., Bautista, B., Huseby, P.G., Li, G., Stern, L.J., and Huseby, E.S. (2011). A role for differential variable gene pairing in creating T cell receptors specific for unique major histocompatibility ligands. Immunity *35*, 694–704.

Streeck, H., Li, B., Poon, A.F., Schneidewind, A., Gladden, A.D., Power, K.A., Daskalakis, D., Bazner, S., Zuniga, R., Brander, C., et al. (2008). Immune-driven recombination and loss of control after HIV superinfection. J. Exp. Med. *205*, 1789–1796.

Theodossis, A., Guillonneau, C., Welland, A., Ely, L.K., Clements, C.S., Williamson, N.A., Webb, A.I., Wilce, J.A., Mulder, R.J., Dunstone, M.A., et al. (2010). Constraints within major histocompatibility complex class I restricted peptides: presentation and consequences for T-cell recognition. Proc. Natl. Acad. Sci. USA *107*, 5534–5539.

Tynan, F.E., Reid, H.H., Kjer-Nielsen, L., Miles, J.J., Wilce, M.C., Kostenko, L., Borg, N.A., Williamson, N.A., Beddoe, T., Purcell, A.W., et al. (2007). A T cell receptor flattens a bulged antigenic peptide presented by a major histocompatibility complex class I molecule. Nat. Immunol. *8*, 268–276.

van Bockel, D.J., Price, D.A., Munier, M.L., Venturi, V., Asher, T.E., Ladell, K., Greenaway, H.Y., Zaunders, J., Douek, D.C., Cooper, D.A., et al. (2011). Persistent survival of prevalent clonotypes within an immunodominant HIV gag-specific CD8+ T cell response. J. Immunol. *186*, 359–371.

JVI
Journals.ASM.org

Distinct HIV-1 Escape Patterns Selected by Cytotoxic T Cells with Identical Epitope Specificity

Yuichi Yagita,[a] Nozomi Kuse,[a] Kimiko Kuroki,[b] Hiroyuki Gatanaga,[a,c] Jonathan M. Carlson,[d] Takayuki Chikata,[a] Zabrina L. Brumme,[e,f] Hayato Murakoshi,[a] Tomohiro Akahoshi,[a] Nico Pfeifer,[d] Simon Mallal,[g] Mina John,[g] Toyoyuki Ose,[b] Haruki Matsubara,[b] Ryo Kanda,[b] Yuko Fukunaga,[b] Kazutaka Honda,[a] Yuka Kawashima,[a] Yasuo Ariumi,[a] Shinichi Oka,[a,c] Katsumi Maenaka,[b] Masafumi Takiguchi[a]

Center for AIDS Research, Kumamoto University, Chuo-ku, Kumamoto, Japan[a]; Laboratory of Biomolecular Science, Faculty of Pharmaceutical Sciences, Hokkaido University, Kita-ku, Sapporo, Japan[b]; AIDS Clinical Center, National Center for Global Health and Medicine, Shinjuku-ku, Tokyo, Japan[c]; eScience Group, Microsoft Research, Los Angeles, California[d]; Faculty of Health Sciences, Simon Fraser University, Burnaby BC, Canada[e]; British Columbia Centre for Excellence in HIV/AIDS, Vancouver, BC, Canada[f]; Institute for Immunology & Infectious Diseases, Murdoch University, Murdoch, Western Australia, Australia[g]

Pol283-8-specific, HLA-B*51:01-restricted, cytotoxic T cells (CTLs) play a critical role in the long-term control of HIV-1 infection. However, these CTLs select for the reverse transcriptase (RT) I135X escape mutation, which may be accumulating in circulating HIV-1 sequences. We investigated the selection of the I135X mutation by CTLs specific for the same epitope but restricted by HLA-B*52:01. We found that Pol283-8-specific, HLA-B*52:01-restricted CTLs were elicited predominantly in chronically HIV-1-infected individuals. These CTLs had a strong ability to suppress the replication of wild-type HIV-1, though this ability was weaker than that of HLA-B*51:01-restricted CTLs. The crystal structure of the HLA-B*52:01-Pol283-8 peptide complex provided clear evidence that HLA-B*52:01 presents the peptide similarly to HLA-B*51:01, ensuring the cross-presentation of this epitope by both alleles. Population level analyses revealed a strong association of HLA-B*51:01 with the I135T mutant and a relatively weaker association of HLA-B*52:01 with several I135X mutants in both Japanese and predominantly Caucasian cohorts. An *in vitro* viral suppression assay revealed that the HLA-B*52:01-restricted CTLs failed to suppress the replication of the I135X mutant viruses, indicating the selection of these mutants by the CTLs. These results suggest that the different pattern of I135X mutant selection may have resulted from the difference between these two CTLs in the ability to suppress HIV-1 replication.

HIV-1-specific cytotoxic T cells (CTLs) play an important role in the control of HIV-1 replication (1–8); however, they also select immune escape mutations (9, 10). Population level adaptation of HIV to human leukocyte antigen (HLA) has been demonstrated (11–15), suggesting that HIV-1 can successfully adapt to immune responses previously effective against it.

It is well known that particular mutations can be selected by CTLs specific for a single HIV-1 epitope. On the other hand, studies on HLA-associated HIV-1 polymorphisms have revealed examples of particular mutations associated with multiple HLA class I alleles (16–21), suggesting that the same mutation can be selected by CTLs carrying different specificities in some cases. However, the selection of the same mutation by CTLs specific for different HIV-1 epitopes has rarely been reported. The change from Ala to Pro at residue 146 of Gag (A146P) is a well-analyzed case. A146P is an escape selected by not only HLA-B*57-restricted, ISW9-specific CTLs (22) but also by HLA-B*15:10-restricted and HLA-B*48:01-restricted CTLs (15, 23, 24), although the latter CTLs selected it by different mechanisms. The replacement of Thr with Asn at residue 242 (T242N) of Gag is another case. This mutant is selected by HLA-B*58:01-restricted and HLA-B*57-restricted CTLs specific for the TW10 epitope in HIV-1 clade B- and C-infected individuals (25–27).

The presence of Pol283-8(TAFTIPSI: TI8)-specific, HLA-B*51:01-restricted CTLs is associated with low viral loads in HIV-1-infected Japanese hemophiliacs, supporting an important role in the long-term control of HIV-1 infection (28). We previously showed that the frequency of a mutation at position 135 (I135X) of reverse transcriptase (RT) is strongly correlated with the prevalence of HLA-B*51 among nine cohorts worldwide and that this mutation is selected by Pol283-8(TAFTIPSI: TI8)-specific, HLA-B*51:01-restricted CTLs (15). Of these cohorts, a Japanese one showed the highest frequency of the I135X mutation in HLA-B*51:01 negatives (66% in a Japanese cohort and 11 to 29% in other cohorts). This finding may be explained by the fact that the Japanese cohort has the highest prevalence of HLA-B*51:01 among these cohorts. Another possibility is that this mutation is selected by HIV-1-specific CTLs restricted by other HLA alleles, which are highly frequent among Japanese individuals but infrequent in or absent from other populations. To clarify the latter possibility, we first analyzed the association of the I135X mutation with other HLA class I alleles in a Japanese cohort and found this mutation also to be associated with HLA-B*52:01. We next sought to identify an HLA-B*52:01-restricted CTL epitope including RT135 and found that both HLA-B*51:01 and -B*52:01 can present the same epitope, Pol283-8. Using population level analyses of Japanese and Caucasian cohorts, we identified HLA-B*51:01- and HLA-B*52:01-specific polymorphisms at RT codon 135 (position 8 of this epitope) and characterized differential pathways of escape between these two alleles. In addition, we assessed the *in vitro* ability of HLA-B*52:01- and HLA-B*51:01-restricted CTLs to se-

Received 20 September 2012 Accepted 26 November 2012
Published ahead of print 12 December 2012
Address correspondence to Masafumi Takiguchi, masafumi@kumamoto-u.ac.jp.
Y.Y., N.K., and K.K. contributed equally to this study.
Supplemental material for this article may be found at http://dx.doi.org/10.1128/JVI.02572-12.

doi:10.1128/JVI.02572-12

lect I135X mutants and elucidated the crystal structure of the HLA-B*52:01-Pol283-8 peptide complex.

MATERIALS AND METHODS

Patients. Two hundred fifty-seven chronically HIV-1-infected, antiretroviral-naïve Japanese individuals were recruited for the present study, which was approved by the ethics committees of Kumamoto University and the National Center for Global Health and Medicine, Japan. Written informed consent was obtained from all subjects according to the Declaration of Helsinki.

In addition, HLA-associated immune selection pressure at RT codon 135 was investigated in the International HIV Adaptation Collaborative (IHAC) cohort, comprising >1,200 chronically HIV-infected, antiretroviral-naïve individuals from Canada, the United States, and Western Australia (19). The majority of the IHAC participants were Caucasian, and the HIV subtype distribution was >95% subtype B.

HIV-1 clones. An infectious proviral clone of HIV-1, pNL-432, and its mutant form pNL-M20A (containing a substitution of Ala for Met at residue 20 of Nef) were previously reported (29). Pol283-8 mutant viruses (Pol283-8L, -8T, -8V, and 8R) were previously generated on the basis of pNL-432 (15, 28).

Generation of CTL clones. Pol283-8-specific, HLA-B*52:01-restricted CTL clones were generated from HIV-1-specific, bulk-cultured T cells by limiting dilution in U-bottom 96-well microtiter plates (Nunc, Roskilde, Denmark). Each well contained 200 μl of the cloning mixture (about 1×10^6 irradiated allogeneic peripheral blood mononuclear cells (PBMCs) from healthy donors and 1×10^5 irradiated C1R-B*52:01 cells prepulsed with the corresponding peptide at 1 μM in RPMI 1640 supplemented with 10% human plasma and 200 U/ml human recombinant interleukin-2).

Intracellular cytokine staining (ICS) assay. PBMCs from HIV-1-seropositive HLA-B*52:01$^+$ HLA-B*51:01$^-$ individuals were cultured with each peptide (1 μM). Two weeks later, the cultured cells were stimulated with C1R-B*52:01 cells or those prepulsed with Pol283-8 peptide (1 μM) for 60 min, and then they were washed twice with RPMI 1640 containing 10% fetal calf serum (RPMI 1640-10% FCS). Subsequently, brefeldin A (10 μg/ml) was added. After these cells had been incubated for 6 h, they were stained with an anti-CD8 monoclonal antibody (MAb; Dako Corporation, Flostrup, Denmark), fixed with 4% paraformaldehyde, and then permeabilized with permeabilization buffer. Thereafter, the cells were stained with an anti-gamma interferon (IFN-γ) MAb (BD Bioscience). The percentage of CD8$^+$ cells positive for intracellular IFN-γ was analyzed by using a FACS-Cant II (BD Biosciences, San Jose, CA). All flow cytometric data were analyzed with FlowJo software (Tree Star, Inc., Ashland, OR).

Identification of 11-mer peptide recognized by HLA-B*52:01-restricted CD8$^+$ T cells. We identified an 11-mer peptide recognized by HLA-B*52:01-restricted CD8$^+$ T cells as follows. We stimulated PBMCs from a chronically HIV-1-infected HLA-B*52:01$^+$ donor (KI-069) with a peptide cocktail including overlapping 17-mer peptides covering RT135 and cultured the cells for 14 days. The cells in bulk culture were assessed by performing an ICS assay for C1R-HLA-B*52:01 cells prepulsed with each of these 17-mer peptides. The bulk-cultured cells recognized the target cells prepulsed with two of the 17-mer peptides assessed, Pol17-47 (KDFRKYTAFTIPSINNE) and Pol17-48 (TAFTIPSI NNETPGIRT). Further analysis with 11-mer overlapping peptides covering the Pol17-48 sequence showed that these bulk-cultured cells recognized the target cells prepulsed with Pol11-142 (TAFTIPSINNE) but not those prepulsed with Pol11-143 (FTIPSINNETP).

Assay of cytotoxicity of CTL clones to target cells prepulsed with the epitope peptide or infected with a vaccinia virus–HIV-1 recombinant. The cytotoxicity of Pol283-8-specific, HLA-B*52:01-restricted CTL clones to C1R cells expressing HLA-B*52:01 (C1R-B*52:01), which were previously generated (30), and prepulsed with peptide or infected with a vaccinia virus-HIV-1Gag/Pol recombinant was determined by the standard ^{51}Cr release assay described previously (31). In brief, the infected cells were incubated with 150 μCi $Na_2{}^{51}CrO_4$ in saline for 60 min and then washed three times with RPMI 1640 medium containing 10% newborn calf serum. Labeled target cells (2×10^3/well) were added to each well of a U-bottom 96-well microtiter plate (Nunc, Roskilde, Denmark) with the effector cells at an effector-to-target (E/T) cell ratio of 2:1. The cells were then incubated for 6 h at 37°C. The supernatants were collected and analyzed with a gamma counter. Spontaneous ^{51}Cr release was determined by measuring the number of counts per minute (cpm) in supernatants from wells containing only target cells (cpm spn). Maximum ^{51}Cr release was determined by measuring the cpm in supernatants from wells containing target cells in the presence of 2.5% Triton X-100 (cpm max). Specific lysis was defined as (cpm exp − cpm spn)/(cpm max − cpm spn) × 100, where cpm exp is the number of cpm in the supernatant in the wells containing both target and effector cells.

Enzyme-linked immunospot (ELISPOT) assay. Cryopreserved PBMCs of chronically HIV-1-infected HLA-B*52:01$^+$ individuals were plated in 96-well polyvinylidene plates (Millipore, Bedford, MA) that had been precoated with 5 μg/ml anti-IFN-γ MAb 1-DIK (Mabtech, Stockholm, Sweden). The appropriate amount of each peptide (100 or 10 nM) was added in a volume of 50 μl, and then PBMCs were added at 1×10^5 cells/well in a volume of 100 μl. The plates were incubated for 40 h at 37°C in 5% CO_2 and then washed with phosphate-buffered saline (PBS) before the addition of biotinylated anti-IFN-γ MAb (Mabtech) at 1 μg/ml. After the plates had been incubated at room temperature for 100 min and then washed with PBS, they were incubated with streptavidin-conjugated alkaline phosphatase (Mabtech) for 40 min at room temperature. Individual cytokine-producing cells were detected as dark spots after a 20-min reaction with 5-bromo-4-chloro-3-indolylphosphate and nitroblue tetrazolium by using an alkaline phosphatase-conjugate substrate (Bio-Rad, Richmond, CA). The spots were counted by an Eliphoto-Counter (Minerva Teck, Tokyo, Japan). PBMCs without peptide stimulation were used as a negative control. Positive responses were defined as those greater than the mean of the negative-control wells plus 2 standard deviations (SD) (the number of spots in wells without peptides).

HIV-1 replication suppression assay. The ability of HIV-1-specific CTLs to suppress HIV-1 replication was examined as previously described (32). CD4$^+$ T cells isolated from PBMCs derived from an HIV-1-seronegative individual with HLA-B*52:01, HLA-B*51:01, or both were cultured. After the cells had been incubated with the desired HIV-1 clones for 4 h at 37°C, they were washed three times with RPMI 1640-10% FCS medium. The HIV-1-infected CD4$^+$ T cells were then cocultured with Pol283-8-specific CTL clones. From day 3 to day 7 postinfection, culture supernatants were collected and the concentration of p24 antigen (Ag) in them was measured by use of an enzyme-linked immunosorbent assay kit (HIV-1 p24 Ag ELISA kit; ZeptoMetrix).

HLA stabilization assay with RMA-S cells expressing HLA-B*52:01 or HLA-B*51:01. The peptide-binding activity of HLA-B*52:01 or HLA-B*51:01 was assessed by performing an HLA stabilization assay with RMA-S cells expressing HLA-B*52:01 (RMA-S-B*52:01) or HLA-B*51:01 (RMA-S-B*51:01) as described previously (33). Briefly, RMA-S-B*51:01 and RMA-S-B*52:01 cells were cultured at 26°C for 16 to 24 h. The cells (2×10^5) in 50 μl of RPMI 1640 supplemented with 5% FCS (RPMI–5% FCS) were incubated at 26°C for 3 h with 50 μl of a solution of peptides at 10^{-3} to 10^{-7} M and then at 37°C for 3 h. After having been washed with RPMI–5% FCS, the cells were incubated for 30 min on ice with an appropriate dilution of TP25.99 MAb. After two washings with RPMI–5% FCS, they were incubated for 30 min on ice with an appropriate dilution of fluorescein isothiocyanate (FITC)-conjugated anti-mouse Ig antibodies. Finally, the cells were washed three times with RPMI–5% FCS and the fluorescence intensity of the cells was measured by the FACS-Cant II. Relative mean fluorescence intensity (MFI) was calculated by subtracting the MFI of cells not peptide pulsed from that of the peptide-pulsed ones.

Sequencing of plasma RNA. Viral RNA was extracted from the plasma of chronically HIV-1-infected Japanese individuals by using a QIAamp

Mini Elute Virus spin kit (Qiagen). cDNA was synthesized from the RNA with Superscript II and random primer (Invitrogen). We amplified HIV RT and integrase sequences by nested PCR with RT-specific primers 5′-CCAAAAGTTAAGCAATGGCC-3′ and 5′-CCCATCCAAAGGAATGGAGG-3′ or 5′-CCTTGCCCCTGCTTCTGTAT-3′ for the first-round PCR and 5′-AGTTAGGAATACCACACCCC-3′ and 5′-GTAAATCCCCACCTCAACAG-3′ or 5′-AATCCCCACCTCAACAGAAG-3′ for the second-round PCR and integrase-specific primers 5′-ATCTAGCTTTGCAGGATTCGGG-3′ and 5′-CCTTAACCGTAGTACTGGTG-3′ or 5′-CCTGATCTCTTACCTGTCC-3′ for the first-round PCR and 5′-AAAGGTCTACCTGGCATGGG-3′ or 5′-TTGGAGAGCAATGGCTAGTG-3′ and 5′-AGTCTACTTGTCCATGCATGGC-3′ for the second-round PCR. PCR products were sequenced directly or cloned with a TOPO TA cloning kit (Invitrogen) and then sequenced. Sequencing was done with a BigDye Terminator v1.1. cycle sequencing kit (Applied Biosystems) and analyzed by an ABI PRISM 310 Genetic Analyzer.

Statistical analysis with phylogenetically corrected odds ratios. Strength of selection was measured by using a phylogenetically corrected odds ratio as previously described (19). Briefly, the odds of observing a given amino acid (e.g., 135V) was modeled as $P/(1-P) = (a \times X) + (b \times T)$, where P is the probability of observing 135V in a randomly selected individual, X is a binary (0/1) variable representing whether or not an individual expresses the HLA allele in question (e.g., B*52:01), and T equals 1 if the transmitted/founder virus for that individual carried 135V and −1 otherwise. Because the transmitted/founder virus is unknown, we averaged over all possibilities by using weights informed by a phylogeny that was constructed from the RT sequences of all of the individuals in the study. The parameters a and b were determined by using iterative maximum-likelihood methods. The maximum-likelihood estimate of a is an estimate of the natural logarithm of the odds ratio of observing 135V in individuals expressing X versus individuals not expressing X, conditioned on the individuals' (unobserved) transmitted/founder virus. P values are estimated by using a likelihood ratio test that compares the above model to a null model in which a equals 0.

To compare the odds of selection between two cohorts, we modified the phylogenetically corrected logistic regression model to include a cohort term, $Z = X \times Y$, where X is the HLA allele, and Y is a 0/1 variable that indicates cohort membership, yielding $P/(1-P) = (a \times X) + (b \times T) + (c \times Z)$, as previously described (19, 34). A P value testing if the odds of escape are different in the two cohorts was estimated by using a likelihood ratio test that compared this model to a null model where c equals 0.

Generation of HLA class I tetramers. HLA class I-peptide tetrameric complexes (tetramer) were synthesized as described previously (31, 35). The Pol283-8 peptide was used for the refolding of HLA-B*51:01 or HLA-B*52:01 molecules. Phycoerythrin (PE)-labeled streptavidin (Molecular Probes) was used for generation of the tetramers.

Tetramer binding assay. HLA-B*51:01-restricted and HLA-B*52:01-restricted CTL clones were stained at 37°C for 30 min with PE-conjugated HLA-B*51:01-tetramer and HLA-B*52:01-tetramer, respectively, at concentrations of 5 to 1,000 nM. After two washes with RPMI 1640 medium supplemented with 10% FCS (RPMI 1640–10% FCS), the cells were stained with FITC-conjugated anti-CD8 MAb at 4°C for 30 min, followed by 7-amino-actinomycin D at room temperature for 10 min. After two more washes with RPMI 1640–10% FCS, the cells were analyzed by the FACS-Cant II flow cytometer. The tetramer concentration that yielded the half-maximal MFI (the EC_{50}) was calculated by probit analysis.

Crystallization, data collection, and structure determination. Soluble HLA-B*52:01 (with beta-2 microglobulin and peptide TAFTIPSI) was prepared as described above. Prior to crystallization trials, HLA-B*52:01 was concentrated to a final concentration of 20 mg ml^{-1} in 20 mM Tris-HCl (pH 8.0) buffer containing 250 mM NaCl. This was done with a Millipore centrifugal filter device (Amicon Ultra-4, 10-kDa cutoff; Millipore). Screening for crystallization was performed with commercially available polyethylene glycol (PEG)-based screening kits, PEGs and PEGs II suites (Qiagen). Thin needle crystals were observed from PEGs II suite 23 (0.2 M sodium acetate, 0.1 M HEPES [pH 7.5], and 20% PEG 3000). Several conditions were further screened by the hanging-drop method with 24-well VDX plates (Hampton Research) by mixing 1.5 μl protein solution and 1.5 μl reservoir to be equilibrated against reservoir solution (0.5 ml) at 293 K. Best crystals were grown from macro seeding with the initial crystals obtained with 0.2 M sodium acetate, 0.1 M Bis Tris propane [pH 7.5], and 20% PEG 3350.

The data set was collected at beamline BL41XU of SPring-8 with Rayonix charge-coupled device detector MX225HE. Prior to diffraction data collection, crystals were cryoprotected by transfer to a solution containing 25% (vol/vol) glycerol and incubation in it for a few seconds, followed by flash cooling. The data sets were integrated with XDS (36) and then merged and scaled by using Scala (37). HLA-B*52:01 crystals belonged to space group $P2_12_12_1$, with unit cell parameters $a = 69.0$ Å, $b = 83.3$ Å, and $c = 170.3$ Å. Based on the values of the Matthews coefficient (V_M) (38), we estimated that there were two protomers in the asymmetric unit with a V_M value of 1.37 $Å^3$/Da (Vsolv = 10.5%). For details of the data collection and processing statistics, see Table S1 in the supplemental material.

The structure was solved by the molecular replacement method with Molrep (39). The crystal structure of HLA-B*51:01 (PDB ID: 1E28) was used as a search model. Structure refinement was carried out by using Refmac5 (40) and phenix (41). The final model was refined to an Rfree factor of 34.7% and an R factor of 29.5% with a root mean square deviation of 0.014 Å in bond length and 1.48° in bond angle for all reflections between resolutions of 38.8 and 3.1 Å. Table S1 in the supplemental material also presents a summary of the statistics for structure refinement. The stereochemical properties of the structure were assessed by Procheck (42) and COOT (43) and showed no residues in the disallowed region of the Ramachandran plot.

Protein structure accession number. Atomic coordinates and structure factors for HLA-B*52:01 have been deposited in the Protein Data Bank under accession code 3W39.

RESULTS

Association of I135X variants with HLA-B*52:01. To clarify the possibility that CTLs restricted by other HLA alleles select the I135X mutation, we investigated the association between other HLA alleles and this mutation in 257 Japanese individuals chronically infected with HIV-1. We found an association of HLA-B*52:01 with the I135X variant, though this association was weaker than that with HLA-B*51:01 (phylogenetically corrected ln odds ratio [lnOR] of 11.76 [$P = 8.77 \times 10^{-4}$] for B*52:01 versus an lnOR of 40.0 [$P = 5.78 \times 10^{-12}$] for B*51:01; Table 1). We also analyzed the effects of HLA-B*52:01 and HLA-B*51:01 in chronically HIV-1-infected Japanese individuals, excluding HLA-B*51:01$^+$ and HLA-B*52:01$^+$ individuals, respectively, and found a significant association between HLA-B*52:01 and I135X variants among 200 HLA-B*51:01-negative individuals with chronic HIV-1 infection ($P = 4.7 \times 10^{-4}$; see Fig. S1A in the supplemental material) and that of HLA-B*51:01 with the variants in 202 HLA-B*52:01-negative ones ($P = 5.3 \times 10^{-8}$; see Fig. S1B in the supplemental material). These results together imply that HLA-B*52:01-restricted CTLs selected this mutation.

Identification of HLA-B*52:01-restricted, Pol283-specific CTLs. To identify the HLA-B*52:01-restricted HIV-1 epitope including RT135, we first investigated whether overlapping peptides covering RT135 could elicit CD8$^+$ T cells specific for these peptides in chronically HIV-1-infected individuals. We identified CTLs recognizing the Pol11-142 (TAFTIPSINNE) peptide in a chronically HIV-1-infected HLA-B*52:01$^+$ donor, KI-069 (see Materials and Methods). Since the C terminus of HLA-B*52:01-binding peptides is known to be a hydrophobic residue (30, 44), we speculated that TAFTIPSI (Pol283-8) was the epitope peptide.

TABLE 1 HLA-B*52:01 and HLA-B*51:01 association with variation at RT135 in Japanese and Caucasian cohorts

HLA class I allele	RT135 target variable	PlyloLOR[a]		Within-cohort *P* value		*P* value comparing cohorts
		Japanese	IHAC	Japanese	IHAC	
B*51:01	T	13.70	4.53	4.66×10^{-6}	1.70×10^{-35}	0.042
B*52:01	T	−9.77	1.25	0.464	2.04×10^{-3}	0.62
B*51:01	I	−40.00	−5.71	5.78×10^{-12}	1.58×10^{-51}	0.052
B*52:01	I	−11.76	−3.06	8.77×10^{-4}	2.95×10^{-5}	0.52
B*51:01	V	−9.76	8.52	0.884	0.41	0.85
B*52:01	V	12.21	10.15	0.076	1.82×10^{-3}	0.037
B*51:01	R	12.08	13.02	0.038	2.36×10^{-3}	0.42
B*52:01	R	0.26	8.37	0.423	0.469	0.89
B*51:01	L	−0.89	3.21	1	0.038	0.17
B*52:01	L	−0.56	3.61	1	0.231	0.29
B*51:01	K	−0.71	−40.00	1	0.53	0.99
B*52:01	K	−0.69	−40.00	1	0.779	0.99
B*51:01	M	7.76	12.00	0.894	2.10×10^{-4}	0.34
B*52:01	M	11.09	−40.00	0.034	0.517	0.12

[a] PlyloLOR, phylogenetically corrected lnOR.

Indeed, bulk-cultured T cells that had been cultured for 2 weeks after stimulation with Pol17-48 recognized C1R-B*52:01 cells prepulsed with Pol283-8 peptide at a much lower concentration than those incubated with the Pol11-142 peptide (Fig. 1A), strongly suggesting that Pol283-8 is an epitope recognized by HLA-B*52:01-restricted CTLs. These findings were confirmed by ELISPOT assay with PBMCs from two HLA-B*52:01$^+$ individuals chronically infected with HIV-1 (Fig. 1B). To clarify whether this peptide was processed and presented by HLA-B*52:01, we investigated the killing activity of bulk-cultured T cells against HLA-B*52:01$^+$ target cells infected with a vaccinia virus–HIV-1 Gag/Pol recombinant. They killed target cells infected with this recombinant but not those infected with wild-type vaccinia virus (Fig. 1C), indicating that the Pol283-8 peptide was presented by

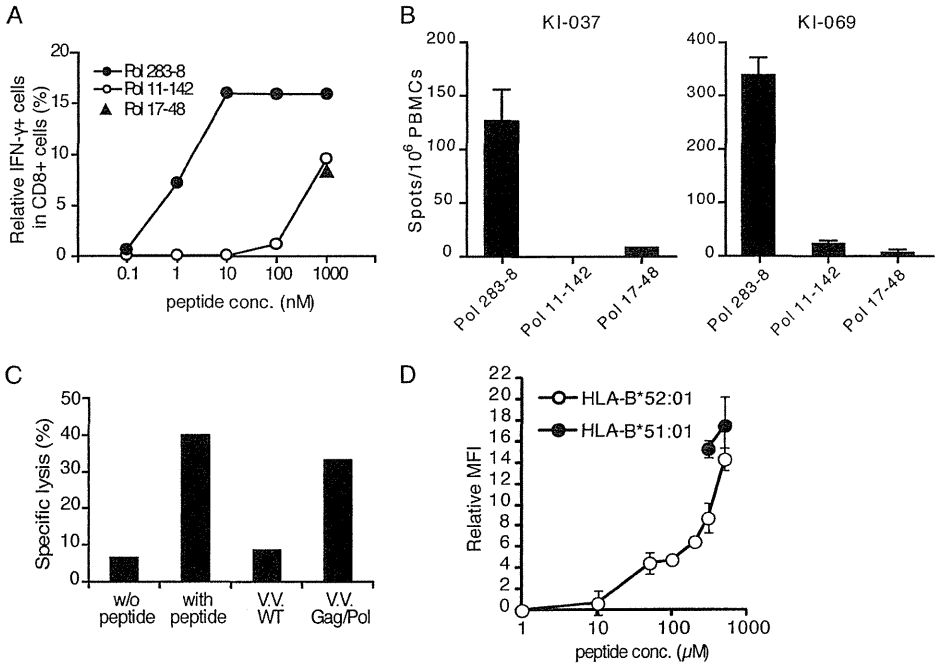

FIG 1 Identification of HLA-B*52:01-restricted Pol epitope. (A) Identification of the epitope peptide recognized by HLA-B*52:01-restricted CD8$^+$ T cells. Bulk T cells were cultured for 2 weeks after stimulation with the Pol17-48 peptide, and then the recognition of C1R-HLA-B*52:01 cells prepulsed with Pol17-48, Pol11-142, or Pol283-8 peptide was assessed by ICS assay. (B) Pol283-8 peptide recognition by T cells *ex vivo*. Recognition of the Pol17-48, Pol11-142, or Pol283-8 peptide by PBMCs from two HLA-B*52:01$^+$ individuals chronically infected with HIV-1 (KI-037 and KI-069) was analyzed by ELISPOT assay. A 100 nM concentration of each peptide was used. (C) Killing activity of Pol283-specific, HLA-B*52:01-restricted CD8$^+$ T cells against cells infected with a vaccinia virus–HIV-1 Gag/Pol recombinant. The killing activities of bulk-cultured T cells stimulated with Pol11-142 against target cells infected with a vaccinia virus–HIV-1 Gag/Pol recombinant (Gag/Pol) and against those infected with wild-type vaccinia virus (V.V. WT) are shown. (D) Binding of Pol283-8 peptide to HLA-B*52:01. Binding ability was measured by performing the HLA class I stabilization assay with RMA-S-B*52:01. RMA-S-B*51:01 cells were used as control cells for the Pol283-8 peptide.

TABLE 2 Pol283-8-specific $CD8^+$ T cells in chronically HIV-1-infected, HLA-B*52:01^+ individuals

Patient ID	HLA class I alleles		No. of CD4 cells/μl	No. of CD8 cells/μl	Viral load (no. of copies/ml)	Antiretroviral therapy	Relative IFN-γ^+/$CD8^+$ % in ICC assay	No. of spots/10^6 PBMCs in ELISPOT[a] assay
KI-037	A*24:02/−	B*52:01/40:02	465	973	76,000	−	64.1	150
KI-090	A*24:02/−	B*52:01/55:01	606	511	≤50	+	40.2	80
KI-106	A*24:02/33:03	B*52:01/07:01	433	890	≤50	+	1.4	<79
KI-126	A*24:02/31:01	B*52:01/40:01	465	NT[b]	36,000	−	60.4	<79
KI-130	A*24:02/−	B*52:01/07:02	351	1,275	14,000	−	0.0	<79
KI-167	A*24:02/−	B*52:01/54:01	455	909	26,000	−	0.0	<79
KI-067	A*24:02/−	B*52:01/48:01	234	1,198	89,000	−	10.9	<79
KI-071	A*24:02/31:01	B*52:01/40:06	292	1,134	48,000	−	0.7	<79
KI-076	A*02:01/24:01	B*52:01/40:01	136	252	14,000	−	61.0	80
KI-114	A*02:01/24:01	B*52:01/27:04	416	463	≤50	+	0.1	<79
KI-056	A*24:02/−	B*52:01/40:02	290	844	8,200	−	-0.1	<79
KI-108	A*24:02/−	B*52:01/−	373	481	NT	−	1.0	<79
KI-028	A*24:02/26:01	B*52:01/48:01	1,351	811	≤50	+	0.5	<79
KI-069	A*24:02/−	B*52:01/40:06	448	1,631	4,400	−	18.1	790

[a] More than the mean number of negative-control spots + 2 SD was defined as a positive response (positive response, >79 spots).
[b] NT, not tested.

HLA-B*52:01. We analyzed the binding of the Pol283-8 peptide to HLA-B*52:01 by using the HLA stabilization assay. The results demonstrated that this peptide bound to HLA-B*52:01 (Fig. 1D). These results together indicate that the Pol283-8 epitope can therefore be presented by both HLA-B*51:01 and HLA-B*52:01.

We investigated whether Pol283-8-specific $CD8^+$ T cells were elicited predominantly in chronically HIV-1-infected HLA-B*52:01^+ HLA-B*51:01^- individuals. PBMCs from 14 of these individuals were analyzed by ICS assay with Pol283-8 peptide-stimulated culture cells, as well as by ELISPOT assay. The results of the ICS assay showed that 7 of these 14 HLA-B*52:01^+ HLA-B*51:01^- patients had Pol283-specific $CD8^+$ T cells, whereas those of the ELISPOT assay with *ex vivo* PBMCs revealed that Pol283-specific $CD8^+$ T cells were detected in only four individuals (Table 2). These results suggest that the three individuals in whom the specific CTLs were detected by the ICS assay but not by the ELISPOT assay may have memory T cells. These results together indicate that Pol283-8 was recognized as an HLA-B*52:01-restricted immunodominant epitope in the HLA-B*52:01^+ individuals and support the idea that the I135X mutation was selected by HLA-B*52:01-restricted, Pol283-8-specific $CD8^+$ T cells.

Strong ability of HLA-B*52:01-restricted, Pol283-8-specific $CD8^+$ T cells to suppress HIV-1 replication. A previous study showed that HLA-B*51:01-restricted, Pol283-8-specific T cells have a strong ability to kill HIV-1-infected target cells and to suppress HIV-1 replication (31). Therefore, we expected that the HLA-B*52:01-restricted T cells also would have this strong ability. We generated HLA-B*52:01-restricted, Pol283-8-specific T cell clones and investigated their ability to kill peptide-pulsed or HIV-1-infected target cells. Clone 1E1 effectively killed C1R-B*52:01 cells prepulsed with the Pol283-8 peptide (Fig. 2A) and NL-432-infected $CD4^+$ T cells from an HLA-B*52:01^+ individual (Fig. 2B). Additional T cell clones also showed strong killing activity against NL-432-infected HLA-B*52:01^+ $CD4^+$ T cells (data not shown). In addition, we investigated the ability of these CTL clones to suppress HIV-1 replication. $CD4^+$ T cells derived from an HLA-B*52:01^+ individual were infected with NL-432 or M20A mutant virus, the latter of which has an amino acid substitution at position 20 of Nef and lacks the ability to downregulate the surface expression of HLA-A and -B molecules (Fig. 2C). Representative data on the 1E1 clone and summary data on four clones are shown in Fig. 2D and E, respectively. These CTL clones strongly suppressed the replication of both the NL432 and M20A mutant viruses, indicating that the HLA-B*52:01-restricted CTLs had a strong ability to suppress HIV-1 replication, as was the case with the HLA-B*51:01-restricted ones.

Recognition of I135X mutations by Pol283-8-specific, HLA-B*52:01-restricted CTLs. Four mutations (8T, 8L, 8R, and 8V) were observed predominantly at RT135 in chronically HIV-1-infected HLA-B*52:01^+ individuals (Fig. 3). These mutations may have been selected by Pol283-8-specific, HLA-B*52:01-restricted CTLs in these patients. We therefore investigated the ability of HLA-B*52:01-restricted CTLs to suppress the replication of these mutant viruses *in vitro*. The CTL clones failed to suppress the replication of the 8L, 8T, or 8R mutant, though they weakly suppressed that of the 8V virus at an E/T cell ratio of 1:1 (Fig. 4A). These results support the idea that these variants were escape mutations from the HLA-B*52:01-restricted CTLs. To clarify the mechanism by which the CTL clones failed to suppress the replication of these mutant viruses, we investigated the CTL clones for recognition of C1R-B*52:01 cells prepulsed with the mutant peptides. The CTL clones effectively recognized the 8V peptide at the same level as the wild-type peptide and the 8T and 8L peptides at less than that of the wild-type one, whereas they failed to recognize the 8R peptide (Fig. 4B). An ELISPOT assay with *ex vivo* PBMCs from KI-069 showed that Pol283-8-specific CTLs effectively recognized the 8I and 8V variants but not the other three mutant peptides (Fig. 4C), suggesting that Pol283-8-specific CTLs failed to recognize the 8T, 8L, and 8R peptides *in vivo*. The lack of recognition of these mutants by CTLs may be attributable to a failure of T cell receptor (TCR) recognition, the inability of the peptide to bind to HLA-B*52:01, and/or disruption of the processing of the epitope in HIV-1-infected cells.

Different pattern of RT135 mutation selection by two HLA alleles. As described above, HLA-B*51:01 and HLA-B*52:01 were associated with I135X in a Japanese population in which the prevalence of HLA-B*51:01 and B*52:01 alleles is relatively high (21.9 and 21.1%, respectively). In a Japanese cohort, out of the five

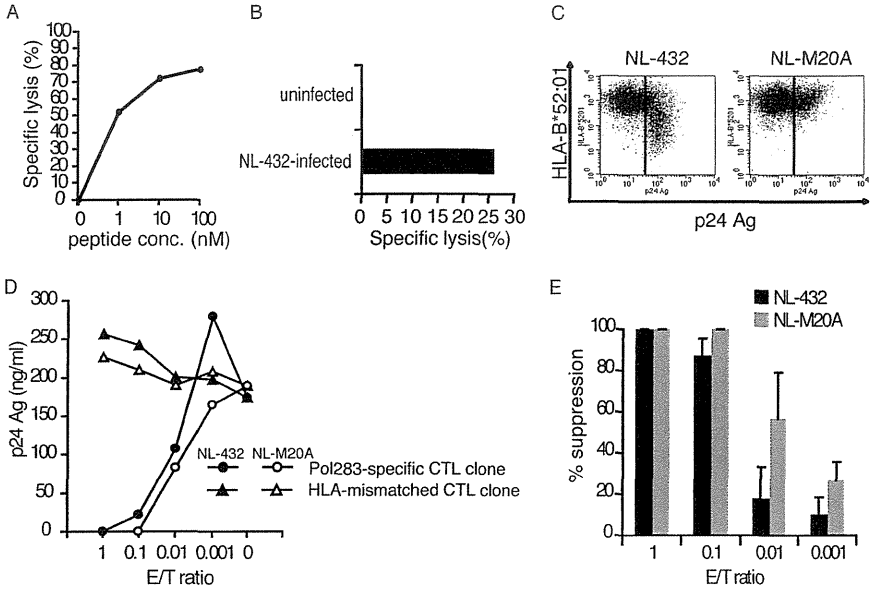

FIG 2 Abilities of HLA-B*52:01-restricted, Pol283-8-specific CD8$^+$ T cell clones to kill HIV-1-infected CD4$^+$ T cells and to suppress HIV-1 replication. (A) Killing activity of an HLA-B*52:01-restricted, Pol283-8-specific CD8$^+$ T cell clone against C1R-B*52:01 cells prepulsed with Pol283-8 peptides. The activity of an HLA-B*52:01-restricted, Pol283-8-specific CD8$^+$ T cell clone, 1E1, to kill C1R-B*52:01 cells was measured by performing a ^{51}Cr-release assay. (B) Killing activity of HLA-B*52:01-restricted, Pol283-8-specific CD8$^+$ T cell clone 1E1 against CD4$^+$ T cells infected with HIV-1. The ability of the clone to kill CD4$^+$ T cells infected with NL-432 was measured by performing a ^{51}Cr-release assay. (C) Downregulation of HLA-B*52:01 in HIV-1-infected CD4$^+$ T cells. CD4$^+$ T cells derived from an HLA-B*52:01$^+$ donor (HLA-A*11:01/A*24:02, HLA-B*52:01/B*52:01, and HLA-C*12:02/C*14:02) were infected with NL-432 and then cultured for 4 days. The cultured CD4$^+$ T cells were stained with anti-p24 Ag and TÜ109 anti-Bw4 MAbs. (D) Ability of an HLA-B*52:01-restricted, Pol283-8-specific CD8$^+$ T cell clone to suppress the replication of NL-432 and M20A mutant viruses. Suppressing ability was measured at four different E/T cell ratios (1:1, 0.1:1, 0.01:1, and 0.001:1). HIV-1-infected HLA-B*52:01$^+$ CD4$^+$ T cells were cocultured with an HLA-B*52:01-restricted, Pol283-8-specific CTL clone or an HLA-mismatched CTL clone at various E/T cell ratios. HIV-1 p24 Ag levels in the supernatant were measured on day 6 postinfection. (E) Summary of the ability of HLA-B*52:01-restricted, Pol283-8-specific CD8$^+$ T cell clones ($n = 4$) to suppress the replication of Nl-432 and M20A mutant viruses at four different E/T cell ratios.

amino acid mutations that can be generated by a one-nucleotide mutation from Ile, the T mutation was strongly associated with the presence of HLA-B*51:01 ($P = 4.66 \times 10^{-6}$), whereas HLA-B*52:01 was associated not with any single amino acid substitu-

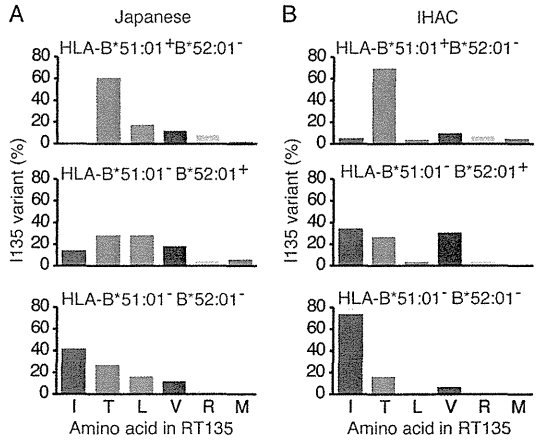

FIG 3 Amino acid variation at RT135 in Japanese individuals. (A) Frequency of the amino acid at RT135 in 51 HLA-B*51:01$^+$ HLA-B*52:01$^-$, 49 HLA-B*51:01$^-$ HLA-B*52:01$^+$, and 151 HLA-B*51:01$^-$ HLA-B*52:01$^-$ Japanese subjects. (B) Frequency of the amino acid at RT135 in 131 HLA-B*51:01$^+$ HLA-B*52:01$^-$, 26 HLA-B*51:01$^-$ HLA-B*52:01$^+$, and 1195 HLA-B*51:01$^-$ HLA-B*52:01$^-$ subjects in three predominantly Caucasian cohorts from Canada, the United States, and Western Australia (IHAC).

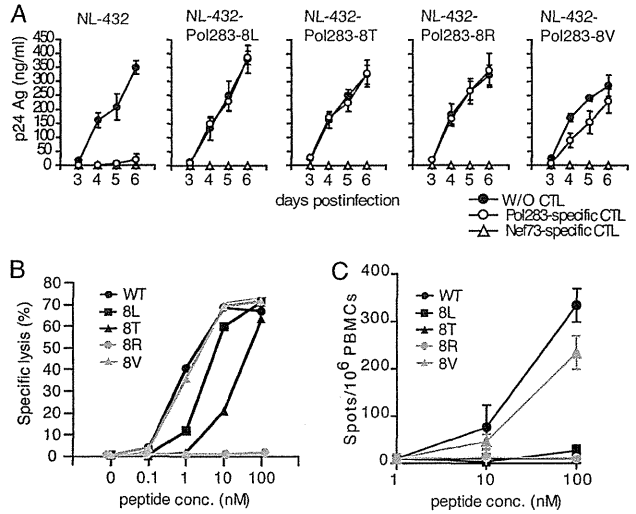

FIG 4 Ability of HLA-B*52:01-restricted, Pol283-8-specific CD8$^+$ T cell clones to suppress the replication of four mutant viruses. (A) Ability of an HLA-B*52:01-restricted, Pol283-8-specific CD8$^+$ T cell clone to suppress the replication of four (8L, 8T, 8R, and 8V) mutant viruses and NL-432. The abilities of an HLA-B*52:01-restricted, Pol283-8-specific CD8$^+$ T cell clone and an HLA-A*1101-restricted Nef73-specific T cell clone to suppress the replication of these viruses were measured at an E/T cell ratio of 1:1 on days 3 to 6. W/O, without. (B) Recognition by an HLA-B*52:01-restricted, Pol283-8-specific CD8$^+$ T cell clone of C1R-B*52:01 cells prepulsed with any one of the four mutant epitope peptides or the wild-type (WT) peptide (8I). (C) Recognition of mutant epitope peptides by *ex vivo* Pol283-8-specific CTLs. The recognition of the Pol283-8 peptide (WT) or the mutant epitope peptide by PBMCs from KI-069 was analyzed by ELISPOT assay.

tion but only with the non-I mutation ($P = 8.77 \times 10^{-4}$, Table 1). The distribution of amino acid variations at RT135 in the HLA-B*51:01$^+$ HLA-B*52:01$^-$ Japanese subjects was different from that in the HLA-B*51:01$^-$ HLA-B*52:01$^+$ ones (Fig. 3). These results suggest that the HLA-B*51:01-restricted CTLs strongly selected the 135T mutation but that the HLA-B*52:01-restricted ones selected a variety of different amino acids at this position in Japanese individuals.

We also analyzed the association of I135X mutations with HLA-B*52:01 and HLA-B*51:01 in three predominantly Caucasian cohorts from Canada, the United States, and Western Australia (International HIV Adaptation Collaborative [IHAC]) (19) comprising >1,200 subjects (Table 1). HLA-B*51:01 was very strongly associated with the I135X mutation (lnOR of 5.71; $P = 1.58 \times 10^{-51}$). Although only 2.1% of the IHAC cohort subjects expressed HLA-B*52:01, this allele was also associated with I135X (lnOR of 3.06; $P = 2.95 \times 10^{-5}$). The T mutation was strongly associated with HLA-B*51:01 ($P = 1.70 \times 10^{-35}$), whereas the T and V mutations were weakly associated with HLA-B*52:01 ($0.0005 < P < 0.005$). Thus, these results showed a similar selection of RT135 mutations by HLA-B*52:01 in the predominantly Caucasian cohort, despite a substantially lower frequency of HLA-B*52:01. The magnitude of the strength of selection by HLA-B*52:01 and HLA-B*51:01 on RT135 did not differ significantly between the two cohorts (Table 1). These results indicate that HLA-B*51:01 strongly selected 135T but that HLA-B*52:01 selected a variety of substitutions at this site (designated I135X) in both the Japanese and non-Japanese cohorts.

Comparison of TCR affinity and abilities of HLA-B*51:01-restricted and HLA-B*52:01-restricted CTLs to suppress HIV-1 replication. We investigated the TCR affinity of HLA-B*51:01-restricted and HLA-B*52:01-restricted CTL clones by using tetramers of the HLA-B*51:01-Pol283 peptide and the HLA-B*52:01-Pol283 peptide complex (HLA-B*51:01 and HLA-B*52:01 tetramers, respectively). The TCR affinity of these CTL clones was compared in terms of EC_{50}. The EC_{50} of the HLA-B*51:01-restricted CTL clones was significantly lower than that of the HLA-B*52:01-restricted CTL clones (Fig. 5A), suggesting that the former CTL clones had TCRs with a higher affinity for the ligand than those of the latter clones. These results imply that the HLA-B*51:01-restricted CTL clones could recognize the HIV-1-infected targets more effectively than HLA-B*52:01-restricted ones.

Since CD4$^+$ T cells derived from an HLA-B*52:01 homozygous individual were used in the experiment shown in Fig. 2D and E, the ability of the HLA-B*52:01-restricted CTL clones to suppress the replication of NL-432 may have been overestimated. To evaluate and compare the abilities of HLA-B*51:01-restricted and HLA-B*52:01-restricted CTL clones to suppress the replication of NL-432, we used CD4$^+$ T cells from individuals expressing HLA-B*51:01$^+$/B*52:01$^-$, HLA-B*51:01$^-$/B*52:01$^+$, or HLA-B*51:01$^+$/B*52:01$^+$ (Fig. 5B). Two HLA-B*51:01-restricted CTL clones strongly inhibited the replication of HIV-1 in cultures of NL-432-infected HLA-B*51:01$^+$/B*52:01$^-$ CD4$^+$ T cells but not in those of HLA-B*51:01$^-$/B*52:01$^+$ cells, whereas two HLA-B*52:01-restricted CTL clones strongly inhibited the replication of HIV-1 in cultures of NL-432-infected HLA-B*51:01$^-$/B*52:01$^+$ CD4$^+$ T cells but not in those of HLA-B*51:01$^+$/B*52:01$^-$ cells (Fig. 5B, left and middle). The ability of the HLA-B*51:01-restricted CTL clones to suppress the replication of HIV-1 was greater than that of the HLA-B*52:01-restricted CTL clones. This was confirmed by the experiment with HLA-B*51:01$^+$/B*52:01$^+$ CD4$^+$ T cells (Fig. 5B, right). Although both HLA-B*51:01-restricted and HLA-B*52:01-restricted CTL clones strongly inhibited the replication of HIV-1 in the cultures of NL-432-infected HLA-B*51:01$^+$/B*52:01$^+$ CD4$^+$ T cells, the former clones exhibited a greater ability to suppress the replication of HIV-1 than did the latter cells. These results indicate that the HLA-B*51:01-restricted CTL clones had a stronger ability to suppress HIV-1 replication than the HLA-B*52:01-restricted clones. Taken together, both our *in vitro* and our *in vivo* (population level HLA-association) data suggest that immune pressure on RT135 by HLA-B*51:01-restricted T cells was stronger than that imposed by HLA-B*52:01-restricted cells.

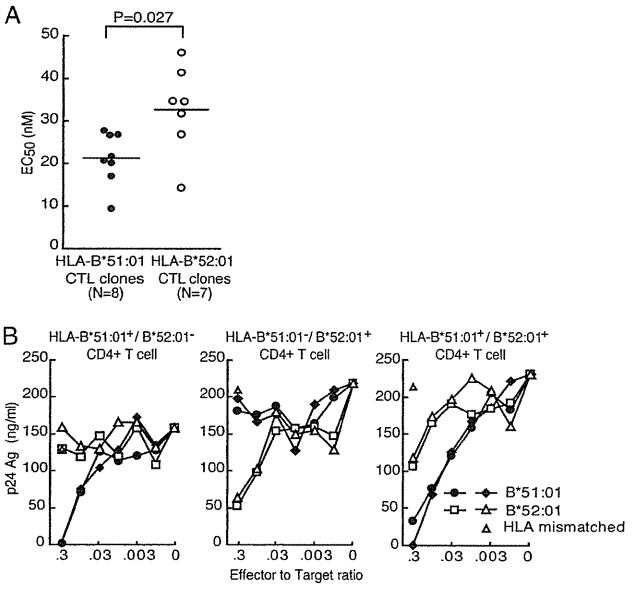

FIG 5 Differences between HLA-B*51:01-restricted and HLA-B*52:01-restricted CD8$^+$ T cell clones in TCR avidity and the ability to suppress HIV-1 replication. (A) TCR avidity of the HLA-B*51:01-restricted and HLA-B*52:01-restricted CTL clones expressed as EC_{50}. The ability of the TCRs of HLA-B*51:01-restricted and HLA-B*52:01-restricted CTL clones to bind HLA-B*51:01 tetramers and HLA-B*52:01 tetramers, respectively, was measured in terms of the MFI of each CTL clone stained with the tetramers at concentrations of 5 to 1,000 nM. (B) The ability of two HLA-B*51:01-restricted and two HLA-B*52:01-restricted CD8$^+$ T cell clones to suppress HIV-1 was measured at six different E/T cell ratios (0.3:1, 0.1:1, 0.03:1, 0.01:1, 0.003:1, and 0.001:1). CD4$^+$ T cells from individuals expressing HLA-B*51:01$^+$/B*52:01$^-$, HLA-B*51:01$^-$/B*52:01$^+$, or HLA-B*51:01$^+$/B*52:01$^+$ were infected with NL-432 and then cocultured with a given Pol283-8-specific CTL clone or an HLA-mismatched CTL clone. HIV-1 p24 Ag levels in the supernatant were measured on day 5 postinfection.

Structural basis of the difference in recognition between HLA-B*52:01- and HLA-B*51:01-restricted CTLs. In order to investigate the structural basis of the difference in recognition between HLA-B*52:01- and HLA-B*51:01-restricted CTLs, we performed a crystallographic study of the HLA-B*52:01 molecule complexed with the Pol283-8 peptide. The recombinant HLA-B*52:01 protein was crystallized, and by using the molecular replacement method, the three-dimensional structure of HLA-B*52:01 complexed with the Pol283-8 peptide was successfully determined. The crystal and statistical data are summarized in Table S1 in the supplemental material. The overall structure and peptide-binding mode were similar to those of HLA-B*51:01 complexed with the same Pol283-8 peptide (Fig. 6A and B), which